IMSE

Institute for Materials Science and Engineering

NONDESTRUCTIVE EVALUATION

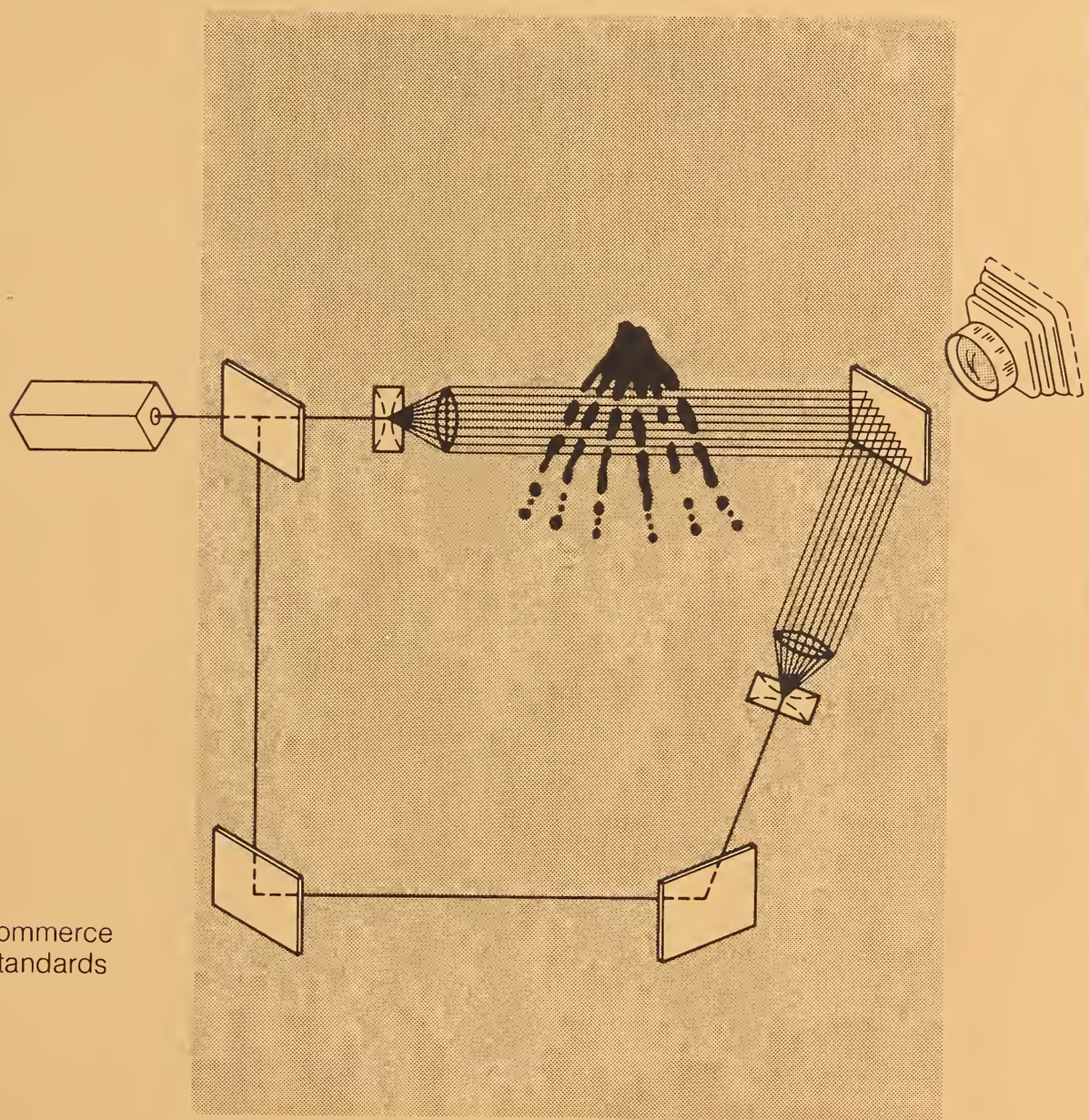

NISTIR 88-3839
U.S. Department of Commerce
National Institute of Standards
and Technology

Technical Activities 1988

Schematic of laser holographic technique that is being used to study the mechanisms of liquid metal breakup into droplets during the intelligent processing of rapidly solidified metal powders. See "Sensors for Metal Powder Atomization Systems" by S.D. Ridder, F.S. Biancaniello, G. E. Mattingly, P. I. Espina, H. G. Semerjian, C. Presser, and T. Hopp in this report.

IMSE

Institute for Materials Science and Engineering

NONDESTRUCTIVE EVALUATION

H. Thomas Yolken, Chief
Leonard Mordfin, Deputy Chief

NISTIR 88-3839
U.S. Department of Commerce
National Institute of Standards and Technology
October 1988

Technical Activities 1988

TECHNICAL ACTIVITIES

Certain commercial equipment, instruments, or materials are identified in this report in order to adequately specify the experimental procedure. In no case does such identification imply recommendation or endorsement by the National Institute of Standards and Technology, nor does it imply that the materials or equipment identified is necessarily the best available for the purpose.

INTRODUCTION

This report provides brief reviews of technical activities in nondestructive evaluation (NDE) that were carried out by or for the National Institute of Standards and Technology (NIST--formerly the National Bureau of Standards) in fiscal year 1988 (October 1, 1987, through September 30, 1988). Collectively, these technical activities constitute the NIST NDE Program that is managed programmatically on a NIST-wide basis by the Office of Nondestructive Evaluation (ONDE).

Traditionally, the most common application of NDE is for the characterization of cracks, voids, inclusions, and other kinds of flaws in materials, components, assemblies, and structures. This usage of NDE is the basis of modern in-service inspection procedures as applied, for example, to aircraft, bridges, pipelines, and pressure vessels. Recognizing that NDE measurements for in-service inspection must be reproducible and quantitative, a key component of the NIST NDE Program is providing traceability for NDE measurements to national measurement standards. To this end, NIST conducts research to achieve an adequate understanding of the physical basis of the NDE measurement techniques and procedures that require standardization. Furthermore, the results of NIST's research and development work on NDE measurements are applied to specific and meaningful problems in order to demonstrate the validity of the results and to help disseminate them to the user communities. Thus, it is possible to think of the NDE Program as comprising three types of activities: research, standardization, and applications.

The most valuable effect of advances in NDE science and technology has been to change NDE from a go/no-go system for the detection of flaws to a quantitative system for the characterization of flaws and also for the nondestructive measurement of material properties and characteristics such as microstructural texture, particle size and agglomeration, polymer cure state, density, surface roughness, etc. The capability for reliable and reproducible nondestructive measurements of this kind is vital to the national effort to raise the quality of manufactured products. Clearly, the ability to monitor important material properties or characteristics during a manufacturing process can often be used to guide or control the process and, thus, to raise both the quality and the uniformity of the product. In recent years, the NDE Program has placed its major emphasis on the application of nondestructive measurement principles to the evaluation of material properties and characteristics and on selected demonstrations of the applicability of these measurements to quality enhancement in the processing of advanced materials.

The reviews in this annual report are arranged in the following sections that reflect the NDE Program's four major activity areas: (1) NDE for Ceramic and Metal Powder Production and Consolidation, (2) NDE for Formability of Metals, (3) NDE for Composites Processing and Interfaces, and (4) NDE Standards and Methods. Each of these sections is preceded by an introduction.

Reports such as this one have been issued on an annual basis since 1978 and are commonly referred to as the "NIST NDE Annual Reports." A parallel series of reports, also issued annually, presents bibliographies and abstracts for the NIST's technical reports and publications on NDE and its supporting technologies. The purpose of both of these report series is to serve as an introduction to NIST's NDE Program. Many readers will want further details on specific aspects of the work or its outputs, and such inquiries are welcomed and encouraged, both by the principal NDE investigators (whose names and affiliation precede each of the articles in the report) and by ONDE. Either can be addressed in care of NIST, Gaithersburg, Maryland 20899 or reached by telephone via (301) 975-2000, FTS 879-2000, or AV 851-1285 ext. 2000. Requests for further information and suggestions regarding the Program always receive prompt and careful attention.

TECHNICAL ACTIVITIES

TABLE OF CONTENTS

I. NDE FOR CERAMIC AND METAL POWDER PRODUCTION AND CONSOLIDATION

This activity is broadly concerned with developing approaches, sensors, and procedures for nondestructively determining those properties of ceramic and metal powders and of consolidated materials that relate to the quality and performance of the materials and manufactured parts. The emphasis is primarily on measurements that can be made during the manufacturing process to sense the pertinent properties of the product during critical stages of its formation and to provide the data required to control the process to optimize quality and productivity. Some of the effort is directed to determining machining damage of ceramic materials. The activity includes development of sensors for metal powder atomization systems; characterization of compacted and sintered ceramics by AC spectroscopy, measurements of the complex dielectric constant by time-domain spectroscopy, and ultrasonic velocity measurements; and determination of machining damage by thermal waves. Although these projects are aimed at developing sensors for the manufacturing process, the project on metal powders represents the most complete approach to this end. It involves the development of a process model, the investigation of a variety of sensors, the study of their performance in an actual inert gas/metal atomization facility, and the development of, and ultimately the use of, an expert system in process control. This project, which is viewed as a model system to obtain experience and insight on how to approach the complete problem of process sensing and control, has been augmented by the formation of an industrial consortium. Representative accomplishments in this activity during the past year include:

- In the program on the metal atomization system, progress was made toward the development of (a) a fundamental understanding of the liquid jet breakup leading to droplet formation, (b) real-time sensing techniques for in situ measurements of droplet size distribution and velocity, and (c) a process model and expert system for the control of the atomization process. (a) A number of flow measurement techniques were tested and evaluated for determining the salient features of the gas and liquid flows. These techniques included Schlieren and high speed photography, pressure and temperature surveys, and optical holography on a number of alloys and fluids. Pulsed holographic studies of the gas-only and gas-liquid flows were initiated for characterizing these flow fields and for photographing single liquid droplets. This work was initiated with water and metal alloys and will be continued with stainless steel (1700 °C). A comparative evaluation of three point measurement techniques for particle sizing in the spray formation region downstream of the atomizer die and in the exhaust stream of its exit section, was performed for liquid sprays. (b) Measurements were made during several stainless steel atomization runs with a laser diffraction technique to obtain a representative measurement of mean particle size and particle size distribution in the atomizer exit section. (c) The design of an intelligent control system has continued. The execution control system on an Amiga computer was completed. The system program loads separate rule-based task modules, supports communication between them, and supports their operation in a multitasking environment. Software that permits interfacing particle size to permit the retrieval of results via a remote computer was developed.

- In the program on the NDE characterization of ceramic sintering, samples were prepared of yttria stabilized ZrO_2, sintered in air at temperatures between 1200° and 1600 °C and annealed from 1 to 5 hours. AC spectra were

obtained on the sintered samples that indicated changes at the grain boundaries and in the grains themselves. Time-domain dielectric measurements made on some of these samples were shown to be consistent and complimentary with the impedance data. Features that are hidden in AC spectroscopy became apparent in dielectric spectroscopy and visa versa. Although the results showed a strong dependence on the process conditions, further work is required to relate the various aspects of both measurements with the specific state of the ceramic such as grain size, interfacial polarization, and density. Finally, preliminary ultrasonic velocity measurements were made on some of the zirconia samples to assess the technique's sensitivity to the firing temperature and time of the ceramic processing. Whereas a definite trend was found that can be explained on the basis of increased densification with sintering time, a consistent relationship with sintering temperature was not observed. To help unravel these results, it would be valuable to determine the porosity of all samples in future tests.

- Thermal wave studies on cutting tools made of hot pressed silicon nitride were conducted to investigate machining damage in these specimens. These samples were subjected to grinding (for 20 minute periods) with decreasing roughness of SiC paper and measured after each grinding period. The average value of the thermal wave signals, when plotted as a function of signal penetration depth, showed definite correlation with the surface damage resulting from the grinding. Although these results are essentially qualitative, they suggest that more quantitative thermal wave measurements may provide a practical, nondestructive method for evaluating damage during machining processes of ceramics.

Sensors for Metal Powder Atomization Systems

S. D. Ridder and F. S. Biancaniello
Metallurgy Division
Institute for Materials Science and Engineering

G. E. Mattingly, P. I. Espina, H. G. Semerjian
and C. Presser
Chemical Process Metrology Division
Center for Chemical Engineering

T. Hopp
Factory Automation Systems Division
Center for Manufacturing Engineering

The research reported here is a continuation of research first supported by ONDE in FY86 that has been aimed at developing an instrumentation system capable of monitoring and controlling atomization processes to achieve the desired particle size distribution. Interest in this project has since attracted support from commercial metal powder producers and users whereby a joint NIST/industrial consortium under ONDE management was initiated in FY88. Work done in FY87 on developing in situ particle size analysis of a gas atomized metal has continued, but with certain modifications due to requirements of the new consortium members. The major changes include (1) dropping the

"low" temperature Sn 5 wt% Sb system and using instead a 304 stainless steel system, which has a significantly higher melting point than the Sn-Sb alloy; and (2) the use of a new "consortium" gas jet die assembly.

The approach taken to develop the required sensor and control system remains the same: (a) a fundamental understanding of liquid jet break-up processes that lead to droplet formation; (b) real-time sensing techniques for in situ measurement of droplet particle size distribution and velocity; and (c) expert systems for control of the atomization process using process models developed in task (a) and particle sensing techniques in task (b).

A. Process and Model Development:

The interactions produced by the specific "consortium" atomization die cause liquid jet instabilities and break-up, followed by droplet formation. The atomization die used in this study produces a circle of supersonic gas jets that impinge on a central, downward flowing, molten liquid metal jet. Detailed characteristics of the supersonic gas flow are critical in determining the nature of the liquid jet break-up and the size of the metal droplets formed. The strategy adopted to produce the desired understanding of these flow processes is to begin with the gas-only flow and continually change conditions and parameters toward the more harsh and hostile conditions present in the actual atomization process.

A range of flow measurement techniques have been tested and evaluated for determining the salient features of these gas and liquid flows including water and metal alloys. Schlieren photography, pressure and temperature surveys, and optical holography have been used to measure and characterize these flows. The waveforms (shown in the FY87 report using Schlieren photography) are due to the gas expansion phenomena. Those distributions may be used to calculate Mach number along the centerline of the jet. When static temperature measurements are made and used to calculate local sound velocities, the Mach number distributions can then be used to calculate local gas velocities. When the liquid jet is present, the gas jet pattern is altered because of the interactions which occur at, and downstream of, the gas-liquid contact point. Upstream of this contact point in the actual atomization process, the gas flow should closely resemble that occurring in the gas-only flow.

Holographic surveys of the gas-only and the gas-liquid flows have been started. This technique offers considerable promise both for characterizing these flow fields and for photographing single liquid droplets. A typical holographic record of the gas-liquid flow in the near jet region is shown in Figure 1. The 20 nanosecond exposure is sufficiently rapid to "freeze" the motion. Also visible in Figure 1 are the contortions on the liquid jet column as well as the density variations in the turbulent gas flow surrounding the liquid. It may be feasible to use pulsed holography to determine drop velocities. In this way both droplet size and speeds can be determined in the gas-liquid flows where this technique can be used.

As previously mentioned the atomizer has been modified to operate at the elevated temperatures necessary to process 304 stainless steel (1700 °C), and a series of atomization runs for repeatability and parameterization data have

commenced using this alloy. Off-line particle size measurement of the powder produced during these runs will be used to determine how gas jet velocity, molten metal superheat, and metal flow rate affect the particle size.

Future activities will include surveys of the pressure and velocity over the cross-section of the gas-only flows. These results will extend our current results obtained along the jet centerline and will produce more complete descriptions of the gas flow field. This will include the oscillations and instabilities present on the outer edges of the gas flow. Holographic surveys and analyses will be continued both to explore the use of this technique in obtaining gas density distributions, the initial break-up mechanisms of the liquid jet column, and the determination of liquid droplet sizes and speeds. The atomization repeatability and parameterization study will be completed in the next year as well as the installation of a higher capacity crucible to allow us to determine steady state conditions.

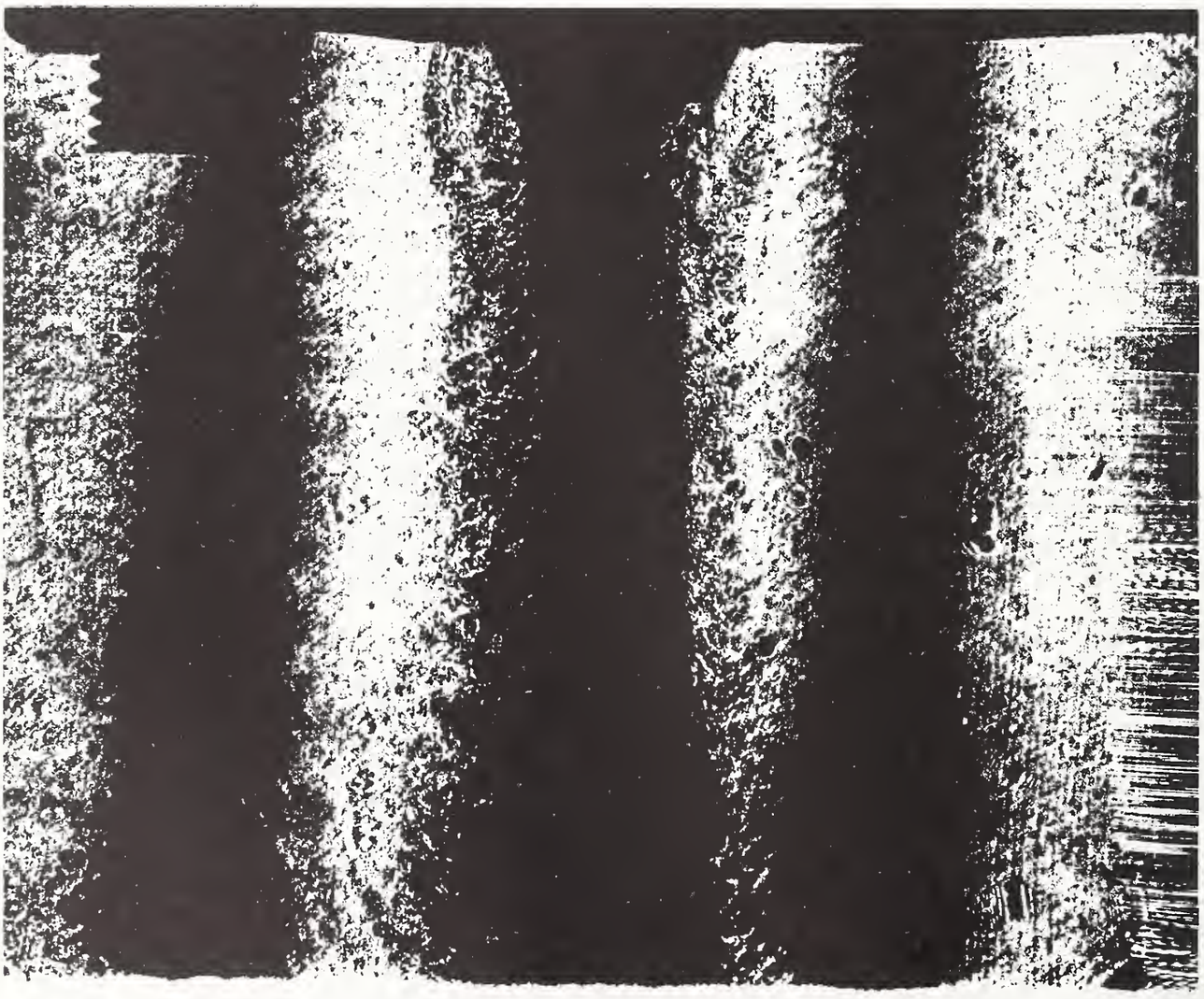

Figure 1. Hologram of water being atomized (20 ns exposure time). Ligament and primary droplet formation are clearly evident.

B. Sensor Development:

Particle sizing techniques are being studied for diagnostics in two sections of the inert gas atomizer facility; viz., (a) in the spray formation region downstream of the atomizer die, and (b) in the exhaust stream of the atomizer exit section. The jet breakup and droplet formation processes in the atomization chamber will be studied by providing detailed measurements of droplet size, number density, and velocity. A comparative evaluation of three-point measurement techniques was performed in previous measurements in liquid sprays; these include (a) polarization ratio, (b) scattering light intensity deconvolution, and (c) phase/Doppler interferometric techniques. Results indicate that the first two techniques are more sensitive to the smaller particle size range ($d < 5$ μm), whereas the third one provides more reliable measurements for larger droplets ($d > 3$ μm).[1] Plans are underway to obtain data with these devices in the liquid-metal atomizer.[2,3] Experiments will be carried out initially with the phase/Doppler instrument, which will be leased within the next several months.

A line-of-sight measurement technique was selected to obtain a representative measurement of mean particle size in the atomizer exit section. The instrument operates on the principle of laser Fraunhofer diffraction, in which particles diffract laser light onto a calibrated multi-element ring diode. The particle size distribution, averaged along a cross section of the process stream, can then be used to determine mean particle size and other statistical properties. The instrument also has the capability to provide input for process feedback and control. The instrument can provide good time resolution for the high process flow rates and particle concentrations, and short run times encountered during atomization (typically 2 min).

To date, measurements were made during several metal atomization runs with the Fraunhofer device. The particle size distribution was generally found to be multimodal and included a wide range of sizes. Sieve measurements for each run indicated that the mean size during a typical run is $D_{0.5} \approx 40$ μm. Discrepancies in these particle sizes can be attributed, in part, to the range detected by each technique, and to coating of the test section windows with a fine layer of metal powder. The window arrangement has been modified to purge argon over the inner window surface; however, a fine layer of powder still coats this surface. Other modifications are currently being studied, but will be carried out in an off-line facility that provides a continuous flow of metal powder.

The continuous metal powder flow facility was used to monitor the response of the laser diffraction apparatus to changes in stream flow conditions; this was accomplished with a pressure-atomized water spray. It was found that as water pressure decreased droplet size increased, as expected; the measured mean droplet diameter matched well the data obtained with a similar laser diffraction instrument, supplied by the nozzle manufacturer. The facility was also used to eliminate laser beam steering effects due to window imperfections and nonparallel surfaces. Currently, fused-silica quartz windows are being used, which enable quick alignment of the laser diffraction instrument at the atomizer test section.

Future activities will include continued operation of the laser diffraction system in the exit section of the atomization chamber. Off-line studies will also be used to evaluate system problems and capabilities, and to carry out a parametric investigation with different metal powders. The phase/Doppler sizing apparatus will be available to obtain data in the metal spray and in the off-line atomization die facility. Experiments will also continue with a laser sheet beam to illuminate the spray jet, and with high speed cinematography to observe the dynamic features of the metal powder spray.

C. Intelligent Control System Development:

In the past year we continued the design of the intelligent controller and implemented several of the supporting services which it will require. In particular, we completed the execution control system (ECS) on the Amiga computer. This program loads separate rule-based task modules, supports communication between them using a common memory implementation, and supports their operation in a multitasking environment.

Currently, the atomization process is controlled and monitored through the Azonix data acquisition system (DAS). An analysis of the project's requirements indicated that the Azonix is inadequate for the real-time control needs of the controller. We have begun to define the specifications for a system to replace the Azonix that will allow direct access to the sensor and control signals. We also developed software routines to interface to the Malvern particle sizer that permit the retrieval of results via a remote computer.

A preliminary version of a controller simulator of the atomization process was demonstrated at the Metal Powder Consortium's annual meeting.

Future activities include acquiring a new DAS, installing the controller computer at the atomizer site, and integrating the DAS system to the atomizer's instrumentation. Based on experiments performed with the installed system, we will refine the implementation of the intelligent controller.

References

1. C. Presser, A. K. Gupta, R. J. Santoro, and H. G. Semerjian, "Laser Diagnostics for Characterization of Fuel Sprays," Proc. 5th Intl. Congress on Appl. of Lasers and Electro-Optics (ICALEO 1986), Vol. 58, pp. 160-167, Arlington, VA (1986).

2. H. G. Semerjian, M. R. Zachariah, and C. Presser, "Laser Diagnostics for Investigation of Particle Formation Processes," presented at the Materials Research Society Spring Meeting, Reno, NV, April 5-9, 1988.

3. C. Presser, "Analysis and Measurement of Process Particles," presented at the Alcoa Laboratories Centennial Symposium on Sensor Technology, Nemacolin Woodlands, PA, June 15, 1988.

Nondestructive Characterization of Ceramic Sintering

J. E. Blendell, J. F. Kelly, and C. K. Chiang
Ceramics Division
Institute for Materials Science and Engineering

G. V. Blessing
Automated Production Technology Division
Center for Manufacturing Engineering

F. I. Mopsik
Polymers Division
Institute for Materials Science and Engineering

The ability to nondestructively monitor the microstructure of a ceramic material during sintering is important for improving the reliability of ceramics. Determining during sintering when the microstructure has achieved a specific condition would allow control of the sintering conditions to reproducibly obtain the desired microstructure. Several techniques including electrical and ultrasonic measurements are being investigated for this purpose.

A. Sample Preparation and Impedance Spectroscopy:

Sintering of ceramics involves the removal of porosity and, at later stages, grain growth. Because grain boundary energy is less than half that of a free surface, initially the system energy is lowered by increasing the area of contact of the grains from point contacts to finite areas. This leads directly to a reduction of porosity. When the pore size is small enough, usually at porosities of less than 10 percent, a further reduction in energy can occur by allowing the grain boundaries to move and with a growth in grain size. While this later stage is occurring, there is a still further reduction in porosity.

To monitor this process, we have previously looked at the use of AC impedance spectroscopy to characterize both the porosity and grain size of a sintered sample. The data showed distinct arcs in the complex resistivity plane that were identified with grain, grain boundary, and electrodes as one goes from high to low frequencies. However, lack of reproducible conditions and well characterized samples prevented a direct correlation with sample microstructure.

To achieve such a correlation, we prepared samples of yttria stabilized ZrO_2, sintered at temperatures between 1200° and 1600 °C in air, annealed for times from 1 to 5 hours. The densities measured, using the geometric volume, varied from 74.4 to 96.7 percent of theoretical density (6.082 gm/cm^3). We are currently measuring the grain size and porosity on polished sections of these samples.

AC impedance spectra were obtained at 350 °C in a dry oxygen atmosphere for samples sintered at 1200° and 1600 °C for both 1 and 5 hours. The electrodes were evaporated platinum. Resistivity arcs previously associated with the bulk grains and the grain boundaries were observed. The results showed a large decrease in magnitude (a factor of 2) in going from 1200° to 1600° with the arc associated with the grain boundaries decreasing the most. This indicated not only a change at the grain boundaries but also in the grains proper.

B. Time-Domain Dielectric Spectroscopy:

Most of the work was aimed at assessing the use of impedance spectroscopy for evaluating the state of Yttria stabilized Zirconia ceramics. Towards this goal, time-domain dielectric measurements were made on some samples that were fired for 1200° and 1600° for 1 and five hours. The samples, with guard rings added, were identical to those used in the impedance measurements. The results, taken at 35 °C for the complex dielectric constant, $\epsilon^* = \epsilon' - i\epsilon''$, in the complex plane, covering seven decades of frequency are shown in Figure 1. The same data were then replotted as impedance spectra (complex resistivity, $\rho^* = \rho' - i\rho''$) using the transformation $\rho^* = 1/(i\omega\epsilon_0\epsilon^*)$ as shown in Figure 2. Instrumental limitations prevented complete determination of the arc to the right. Within the limits of the data, and allowing for the large change in measuring temperature, the results with AC impedance spectroscopy were consistent, were those of dielectric measurements.

For the data measured in this study, it has become clear that both representations can be useful in evaluating the ceramic. The limiting value at high frequencies, ϵ_h, is hidden in a ρ plot. For the samples studied here, ϵ_h was definitely a function of the density, and, for this particular material, also the composition. The low frequency tail of the ϵ'' vs. ϵ' plot, seen in Figure 1 as the beginning of an arc curving to the right, from its magnitude is clearly due to interfacial polarization. The minimum in the ρ'' vs. ρ' plot, clearly seen in Figure 2, maps into the inflection point of the ϵ'' vs. ϵ' plot that is however difficult to find. The minimum in ρ'' vs. ρ' plot corresponds to a bulk conductance that is related to several material properties. This number has a strong dependence on the processing conditions. There also appeared to be some changes in the total data with the changes in the ceramic grains, but the data are still incomplete.

Future work should include an attempt to more rigorously tie together the impedance and dielectric representations of the data. The data are clearly complementary and definitely show promise for sinter monitoring. A more well defined as well as a more important system, Al_2O_3, will allow a more satisfactory comparison. Also, such studies should be conduced with well characterized system, such as alumina, where the basic material properties are well defined.

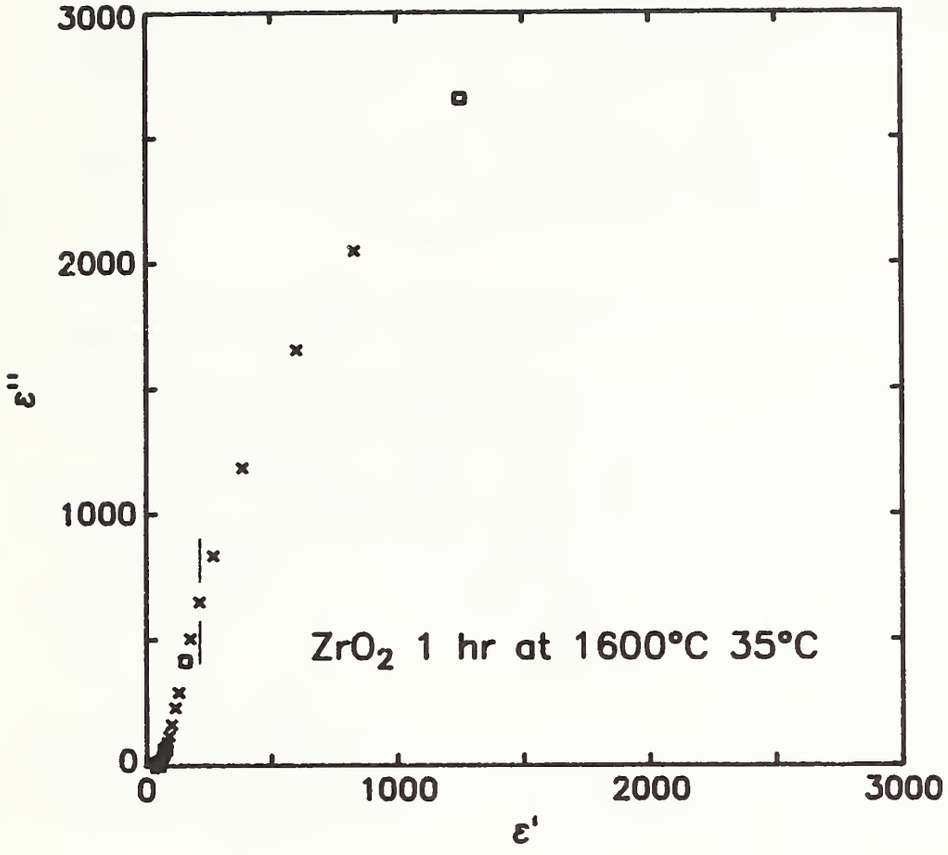

Figure 1. The imaginary component of the complex dielectric constant (ϵ") versus the real component (ϵ') for yttria-stabilized zirconia. Each point is for a given frequency with the decades marked by (□). Frequency decreases from left to right. The marked point corresponds to a similarly marked one in Figure 2.

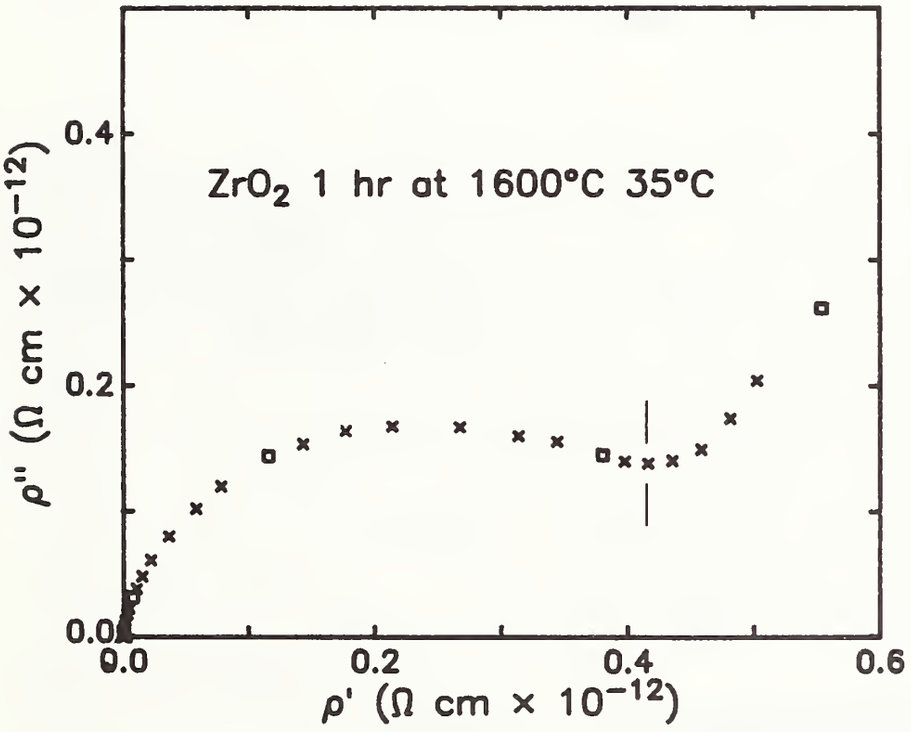

Figure 2. The imaginary component of the complex resistivity (ρ") as a function of the real component (ρ') for yttria-stablized zirconia. The frequency points are marked as in Figure 1 with frequency decreasing to the right.

C. Ultrasonic Velecity Measurements:

Preliminary ultrasonic velocity measurements were made on zirconia samples to assess the technique's sensitivity to specific ceramic process parameters. These parameters were the firing temperature (1400, 1500, and 1600 °C) and the firing time (1 and 5 hrs.), which in combination yielded six distinct process states for the material sample sets. The 1.5 cm diameter samples varied in thickness from 0.5 to 2.8 mm. The thinnest (0.5 to 1.1 mm) and the thickest (1.0 to 2.8 mm) samples were chosen from each of the six sample sets to also evaluate the possible influence of sample volume on processing.

The ultrasonic velocities were determined by measuring the transit-time of short duration (0.1 μs) high frequency (15 MHz) dilational elastic wave pulses echoing between the parallel sample faces. A dry-coupling elastomer was used between the transducer and samples to avoid sample contamination. The velocities, obtained from the ratio of sample thickness to average transit-time using successive echoes, were precise to 0.2 percent. The results on the thick samples are plotted in Figure 3 as a function of firing temperature for the two firing times. Two meaningful trends with implications for process monitoring were observed. (1) The velocity of all samples increased with increasing firing temperature, and (2) the velocity of the longer-fired (5 hrs.) samples were greater in velocity at a given temperature than the shorter-fired (1 hr.) samples. Both trends can be explained on the basis of increased densification with increased sintering time and temperature. The results on the thin samples showed that their velocities also increased with increasing firing temperature. However, a consistent relationship as a function of firing temperature was not observed, possbly due to the unknown sample porosity.

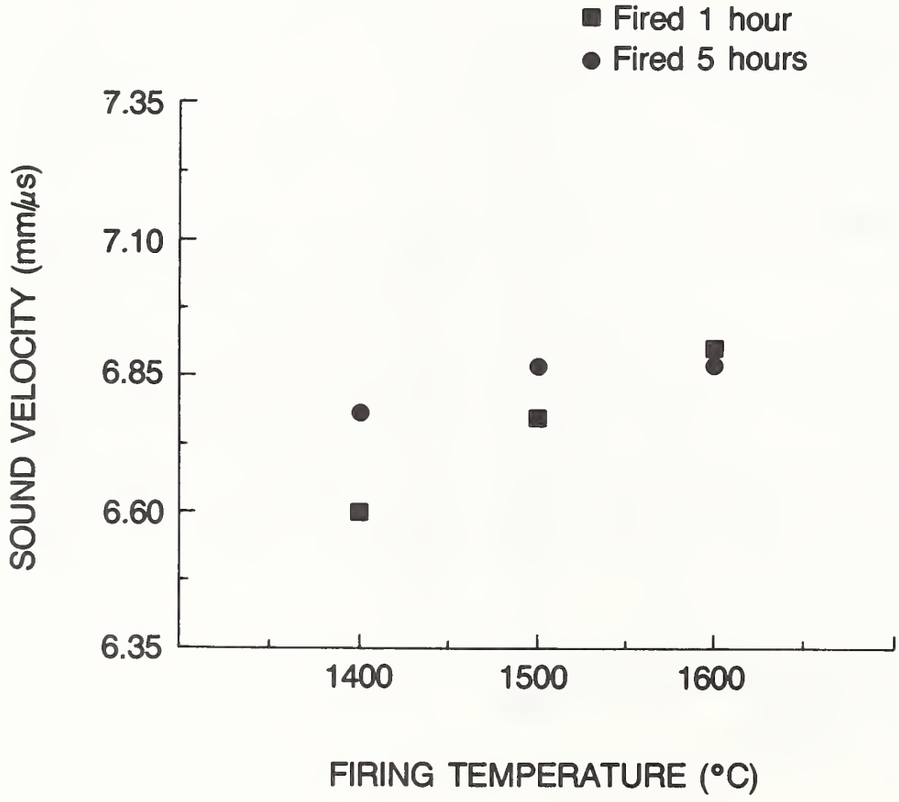

Figure 3. The ultrasonic velocity as a function of firing temperature for two sets of zirconia samples respectively fired for one and five hours.

In conclusion, we note that the ultrasonic velocity, a measure of the material modulus of elasticity, is a sensitive monitor of sample densification as a function of firing time and temperature. To further evaluate this relationship, it would be valuable to precisely determine the porosity of all samples in future tests.

Thermal Wave Studies of Surface Finish (Machining Damage)

G. White
Ceramics Division
Institute for Materials Science and Engineering

The investigation of machining damage effects on high performance ceramics was undertaken with thermal wave measurements; specifically, with the mirage detection technique. The term "thermal waves" is used to describe the diffusion of heat in a material during periodic heating. The resulting thermal signal is sensitive to variations in the thermal properties of the material. The thermal probe length is μ (micrometers), the thermal diffusion length, and is a function of the period, or the modulation frequency, of the heating source

$$\mu = [\alpha/\pi f]^{\frac{1}{2}} \qquad (1)$$

where α is the thermal diffusivity of the specimen and f is the frequency. Because of the critically damped nature of thermal waves, μ also corresponds, to the distance the signal will travel, i.e., changing f corresponds to changing the depth and lateral range of the thermal wave signal. Therefore, the sensitivity to very near surface defects is increased at higher frequency. Accomplishments during FY 1988 are divided into two categories: mirage system improvement and machining damage assessment.

Mirage System Improvement:

Variations in frequency vary the depth that is probed. Previously, frequency was varied manually, greatly restricting the type and range of experiments that were feasible. This year, a function generator and acousto-optic modulator were added to the mirage system, and software was incorporated that allowed computer scanning of the frequency. A second improvement was the development of a method of transferring the data from the system in use to other computers for analysis. Previously, the mirage system was capable of providing a listing of the data or of plotting single frequency curves. However, obtaining multi-frequency curves and statistical analysis of the data was not possible. The ability to transfer the data to computer systems, which already contain data handling software, expands the capability of the mirage system without a major investment in software development. The practical effect of these two changes is that data can now be taken in a day that previously would have required a week.

Machining Damage:

NDE needs in high performance ceramics were discussed with ceramists at the Norton Company. They were particularly concerned with potential damage from

their machining procedures, i.e., cracks, microcracks, and residual stress. Consequently, they provided 12 x 12 x 6 mm hot pressed silicon nitride cutting tool specimens for determining the sensitivity of thermal waves to machining damage. Machining damage in these specimens can be viewed in two ways: first, the damage can be considered as a set of discrete flaws, each of which affects the flow of heat in its vicinity; second, the damage can be viewed as a thin layer of material that has a thermal diffusivity that is different from that of the bulk material. In the first case, effort was directed to detection of individual flaws in the material, particularly on detection of critically large flaws. In the second case, the approach was to consider the damaged layer as a second material and to relate the degree of damage to the degree of change in the thermal behavior of this material.

Two-dimensional maps of specimen surfaces were used to look for discrete damage as a function of surface preparation. To evaluate the material in terms of a uniform damage layer, measurements of the thermal wave signal magnitude and phase from multiple positions on the specimen surface were averaged. In both the discrete and the averaged approaches, measurements were made as a function of frequency to provide depth information. In addition, a third measurement was used that combines the discrete and the average approaches. The standard deviation of the averaged magnitude and phase were calculated and plotted as a function of frequency. This approach recognizes that the damage layer is composed of a large number of discrete flaws and assumes that, as the number and severity of the flaws increases, the standard deviation of the averaged signals will increase. Therefore, as frequency is increased, the probe samples material nearer the surface and, as the damaged region makes up a larger fraction of the material tested, the standard deviation will increase.

The specimens from Norton Company were examined in as-received condition, using all three of the approaches outlined above. They were subjected to grinding for 20 minute periods with decreasing roughness of SiC paper (180, 240, and 320 grit) and remeasured after each grinding period. Figure 1, a three dimensional plot of the phase of a specimen surface after the 240 grit grinding, clearly shows grinding grooves remaining in the material. The as-received material, in contrast, did not exhibit coarse groove structure, but did exhibit other discrete defects ranging from 20 to 110 μm. As Figure 1 shows, such defects would be undetectable after coarse grinding, but would appear as the surface was polished to finer finishes. The average value of the thermal wave signals, when plotted as a function of penetration depth, shows a systematic deviation correlated with the surface damage resulting from grinding. The standard deviation of the thermal wave signals also shows a large increase as the frequency was increased above 500 Hz. These results show that the averaged thermal wave signals are sensitive to the level of grinding.

In addition, thermal diffusivity measurements of the specimen after grinding show a clear change from the bulk value of α. In the as-received specimens, α is constant up to f = 3500 Hz. After grinding with 180 grit paper, the values of α deviate from this value for f > 600 Hz. This deviation decreased after the specimen was ground with 240 grit paper and decreased further after grinding with the 320 grit paper, showing that it was related to the grinding

process. These results are particularly interesting since they do not require an "ideal" specimen for comparison. At low frequencies, the thermal diffusivity is that of the bulk while at higher frequencies, apparently related to the degree of surface damage, α deviates from the bulk value. The amount of deviation increases as the frequency increases.

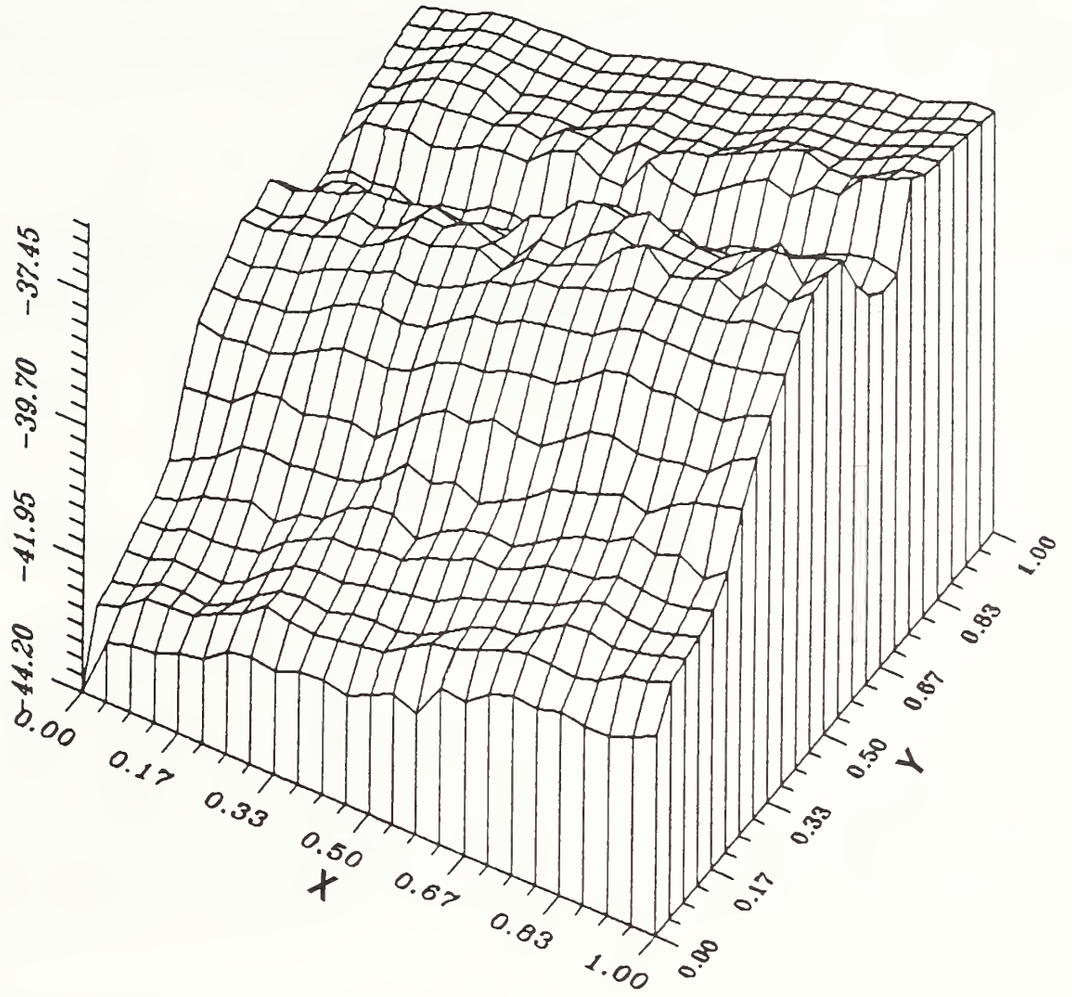

Figure 1. Thermal wave phase measurement of the surface of a hot-pressed silicon nitride specimen showing effects of grinding grooves from 240 grit paper. The horizontal axes are in mm. The vertical axis has arbitrary units.

While the results achieved thus far are qualitative, they suggest that quantitative thermal wave measurements of machining damage may provide a practical method for evaluating damage during machining processes.

Finally, evaluation of the thermal diffusivity of ceramic dielectric specimens, which have undergone different processing treatments, has just begun. Previously, photoacoustic measurements[1] of thermal diffusivity were made on a set of typical barium titanate based capacitor materials. The new set includes specimens that have undergone different firing treatments and that may have lamination defects. The specimens were supplied by the AVX

Corporation as part of a collaborative effort to understand the properties of capacitor materials.

Future work lies in two areas. The first of these is a continuation of the present effort to finer levels of surface damage to find the sensitivity limits of the techniques. The second area is to explore residual stresses that pose a severe problem in ceramics and result from most machining processes. We intend to determine whether thermal wave measurements are sensitive to surface stresses and to relate thermal wave signals to the level of the surface stress.

References:

1. G. S. White, C. Nguyen, and B. Rawal, "Young's Modulus and Thermal Diffusivity Measurements of Barium Titanate Based Dielectric Ceramics," Nondestructive Testing of High-Performance Ceramics, pp. 371-379 (American Ceramic Society, Westerville, OH, 1987).

II. NDE FOR FORMABILITY OF METALS

The goal of this activity in the NDE Program is to develop generic approaches, sensors, and procedures for characterizing metals during the forming process. The emphasis is on measurements that can be made on the production line to improve process control rather than developing inspection techniques for post-manufacturing inspection.

Current efforts in this activity include the development of NDE temperature sensors based on eddy current techniques for determining the internal temperature distribution in hot metal objects, developing an in-process ultrasonic monitor for metal grain texture in manufacturing of steel products, and utilizing ultrasonics for on-line monitoring of both metal surface roughness and cutting tool wear during machining. Representative accomplishments in this activity during the past year include:

- The formability of sheet metal, which in large part depends on grain texture or grain orientation, is a significant process variable in the manufacture of such diverse items as beverage cans, appliances, and automotive panels. In order to improve process control, a noncontacting ultrasonic method was developed last year for on-line monitoring of texture in aluminum sheet. This year's research, in collaboration with the Advanced Steel Processing and Products Research Center, demonstrated that the technique is also applicable to thin ferritic steel sheet.

- The determination of surface roughness during machining of bulk metal parts is desirable for both quality control of the finished product and control of the cutting or grinding process. An ultrasonic NDE sensor was developed two years ago for on-line monitoring of surface finish and last year's research successfully demonstrated that the same ultrasonic sensor could be utilized to detect on-line worn or damaged cutting tools. This year's research shows that a finely focused ultrasonic beam can be used to map the topography of a surface in a fashion analogous to the contacting stylus profilometry technique.

Eddy Current Temperature Sensing

A. H. Kahn, M. L. Mester,* and H. N. G. Wadley
Metallurgy Division
Institute for Materials Science and Engineering

*Research Associate, The Aluminum Association

The principal objective of the NIST-Aluminum Association joint project on temperature measurement is the development of a temperature sensor for control of extrusion processing. In Phase I, the first year of the project (1986-87), an eddy current system was assembled and prepared for testing in plant operation, as described in last year's report. At the end of Phase I the plant test was successfully carried out at the Cressona Aluminum Co., Cressona, PA.

The sensor coil system used for the tests was installed in one quadrant of a four channel canister. The canister was mounted horizontally in the extrusion press and four extrusions passed through it, one through the sensor. In the series of tests a total length of approximately one mile of products passed through the sensor; the temperature was measured and recorded every 1.25 seconds. Figure 1 shows a recording of the data collected during the extrusion of one billet. The breakout temperature is low because the starting metal comes from the cooled end of the billet; the temperature rises with time as the inner part of the billet is extruded and also because the die becomes heated. After 60 seconds the billet was exhausted and the cooling of the static aluminum remaining in the sensor was observed. Figure 2 shows the temperature measurements on a billet for which the speed of extrusion was varied in order to demonstrate the ability of the sensor to follow the temperature under widely varied conditions.

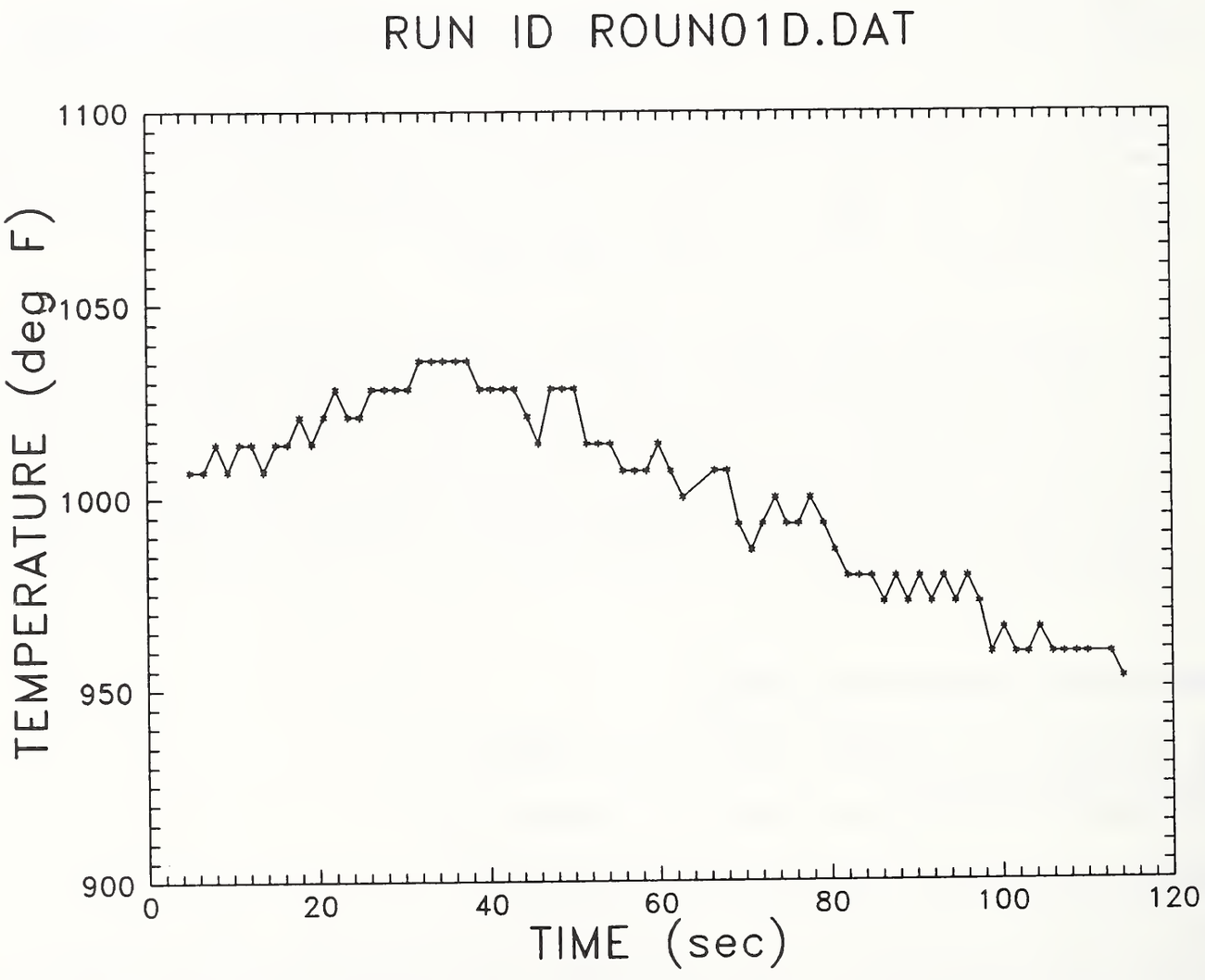

Figure 1. Measured temperature as a function of time for a typical 1-in round aluminum rod during extrusion processing.

In the trials at Cressona the encircling coil described in the previous report was used. This sensor was used for solid round, solid square, and hollow square extrusions. It would also be satisfactory for round tubing.

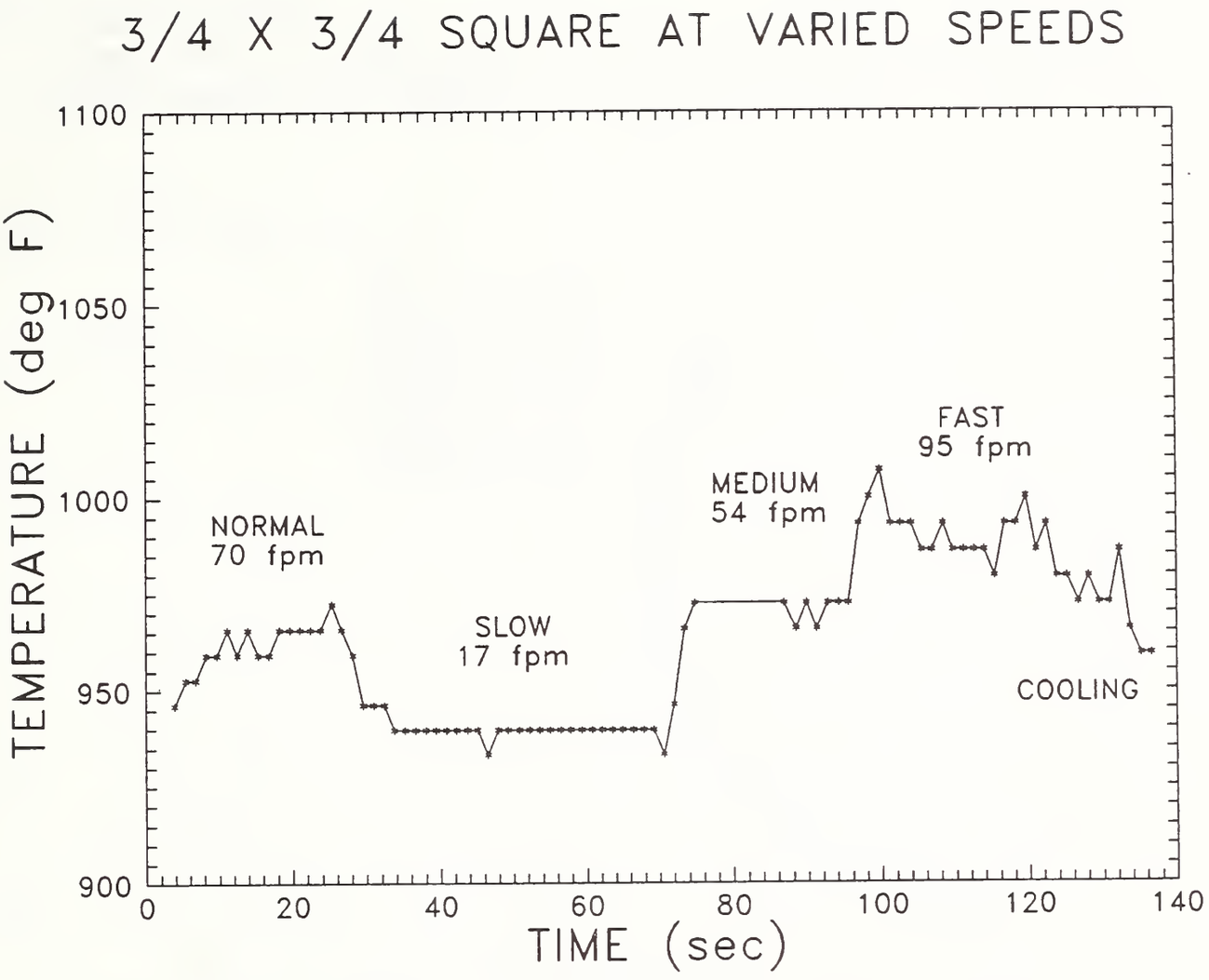

Figure 2. Measured temperature as a function of time for 3/4-in-square aluminum stock during extrusion. The speed was intentionally varied to demonstrate heating effects.

In the Phase II period of this project (1987-88) the eddy current sensor system is being extended to other shapes of interest such as flat strips and sheets, U-channels, and I-beams. In these cases the geometric shape presented for measurement is that of a thin flat wall. An appropriate testing method employs through-transmission techniques in which an exciting coil is placed on one side of the test material and the response of the material is received by a secondary coil on the opposite side. We have prepared a laboratory model of such a coil system for operating at room temperature with test materials of various thicknesses and conductivities, simulating the properties of aluminum products at elevated temperatures. For flat sections of less than a skin depth, the measured complex impedance points for a given coil configuration fall on a single universal curve, with each point corresponding to a unique value of the parameter $X = \sigma\Omega t$, where σ is the electrical conductivity, Ω is the angular frequency, and t is the thickness of the plate. Data taken on the through-transmission system are presented as transfer impedance values, i.e., the ratio of output voltage to input current, with the result divided by the reactance in the absence of the test sample. A plot of through-transmission for several samples of various thicknesses and conductivities at various

frequencies is shown in Figure 3. The tendency of the curves to separate at the high frequency end signifies breakdown of the large skin-depth approximation and is used to establish the limit of validity of the approximation.

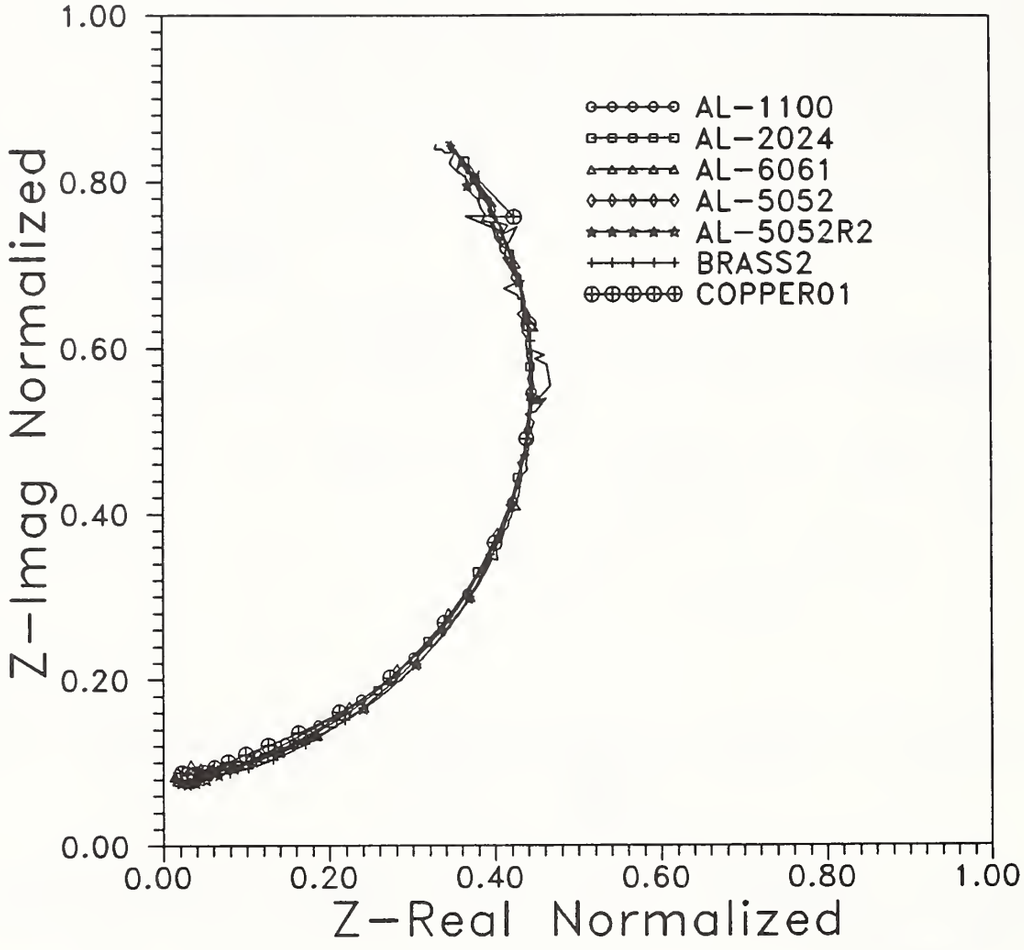

Figure 3. Impedance plane plots of frequency-sweep through-transmission signals measured on seven flat plates of various thicknesses and conductivities. Symbols are placed at every twentieth frequency point for each sample. Each point on the curve corresponds to a unique value of the product of frequency, conductivity, and thickness. In all cases the samples are thin relative to the skin depth.

On the basis of these results, we have designed a set of through-transmission coils for placement in an extrusion canister for on-line testing. Construction of the system in the canister, with water cooling, is now in progress. During the planned tests simultaneous comparison with radiometric methods will be carried out.

NDE for Metal Texture

A. V. Clark
Fracture and Deformation Division
Institute for Materials Science and Engineering

G. V. Blessing
Automated Metrology Division
Center for Manufacturing Engineering

R. B. Thompson
Center for Nondestructive Evaluation
Iowa State University

D. Matlock
Advanced Steel Processing and Products Research Center
Colorado School of Mines

R. C. Reno
Metallurgy Division
Institute for Materials Science and Engineering

The formability of sheet metal is a significant process variable in the manufacture of such diverse items as beverage cans, appliances, and automotive panels. A typical example is press-shop operation in the automotive industry. Here, sheet segments are cut ("blanked") from a coil and fed into a production line. The blanks are then formed into components such as door panels. If variability in material formability occurs, the parts may not have the desired shape. On automated production lines this may result in line shut-down. This may occur because a robot arm is programmed to go to a specific location, grip the part, and move it elsewhere; if the part has the wrong shape, the arm may not be able to secure the part. It appears, especially in the automotive industry, that users of sheet steel will soon be requiring both higher formability and tighter bounds on variation in formability. Therefore, it would be highly desirable to develop a rapid, nondestructive method for characterizing formability of sheet before it enters a production line.

One method in current off-line use is the so-called "modul-r" technique[1] that is based on an experimental correlation between ultrasonic measurement of Young's modulus, E, and a commonly used (destructive) measurement of formability, the r-value. The r-value is typically obtained by cutting tensile coupons at 0°, 45°, and 90° to the rolling direction, and then measuring the ratio:

$$r = \epsilon_{\ell\ell}/(\epsilon_{\ell\ell} + \epsilon_{tt})$$

where $\epsilon_{\ell\ell}$ and ϵ_{tt} are the longitudinal and thickness strains, respectively, at a significant level of plastic deformation. As currently implemented, the "modul-r" method requires small specimens to be cut from the end of a coil (at 0°, 45°, and 90°) and inserted into an ultrasonic instrument that measures E by magnetostrictively inducing a sound wave in the specimen. However, this

approach is destructive, will work only on magnetic materials, and can only be used in a practical sense on specimens removed from the end of a coil.

Since the work of Reference 1 there have been several theories developed that relate velocities of bulk, guided, and surface waves to the texture of polycrystalline, rolled sheets of cubic metals. There also exists a relation between texture (degree of preferred orientation of the polycrystals) and the sheet formability. Consequently, there are now several candidate methods for nondestructive ultrasonic formability measurement.

We have recently been focusing our efforts on the use of noncontacting ultrasonic transducers for both on- and off-line measurement of sheet formability.[2-5] In this work, we are primarily using electromagnetic-acoustic transducers (EMATs) which induce ultrasound in the sheet without the need for an intervening couplant. We have obtained a well-characterized set of steel sheets having a wide range of the average r-value, $\bar{r}$. Measurements of bulk and guided wave arrival times have been made. For bulk waves, we used longitudinal and shear waves propagating through the plate thickness. For guided waves, we used both the lowest-order shear-horizontal wave (SH_0-mode) and the lowest-order symmetrical Lamb wave (S_0-mode). From theory, various combinations of arrival times should be proportional to $\bar{r}$. These combinations are listed in the table below:

Wave Type	Arrival Time Combination
Bulk	$T_\ell/(T_\ell + T_{S1} + T_{S2})$
Guided S_0-mode	$[T(0°) + T(90°) + 2T(45°)]/4$
Guided SH_0-mode	$[T(0°) + T(45°)]/2$

Here T_ℓ, T_{S1} and T_{S2} are arrival times of longitudinal waves and shear waves polarized parallel and perpendicular to the rolling direction. $T(\theta)$ is the arrival time of a guided wave propagating at angle θ to the rolling direction. A comparison of ultrasonic arrival time combinations revealed that all three combinations were indeed proportional to the average drawability $\bar{r}$. An example is shown in Figure 1, where $\langle T_{S0} \rangle$ refers to the arrival time combination for the S_0-mode. The range of $\bar{r}$. in Figure 1 is typical of the drawability desired of sheet for automotive applications.

As mentioned above, the "modul-r" technique relies on the correlation of $\bar{r}$ with $\bar{E}$, the average Young's modulus in the plane of the sheet. There is an approximate relation between the low-frequency limit V_{LIM} of the S_0-mode velocity and the Young's modulus:

$$V_{LIM}^2(\theta) = \frac{E(\theta)}{\rho(1-\nu^2)}$$

Here θ is the angle relative to the sheet rolling direction and ν is Poisson's ratio. The S_0-mode data were analyzed using the above relation, and the $\bar{E}$ calculated from

$$\bar{E} = [E(0°) + E(90°) + 2\ E(45°)]/4$$

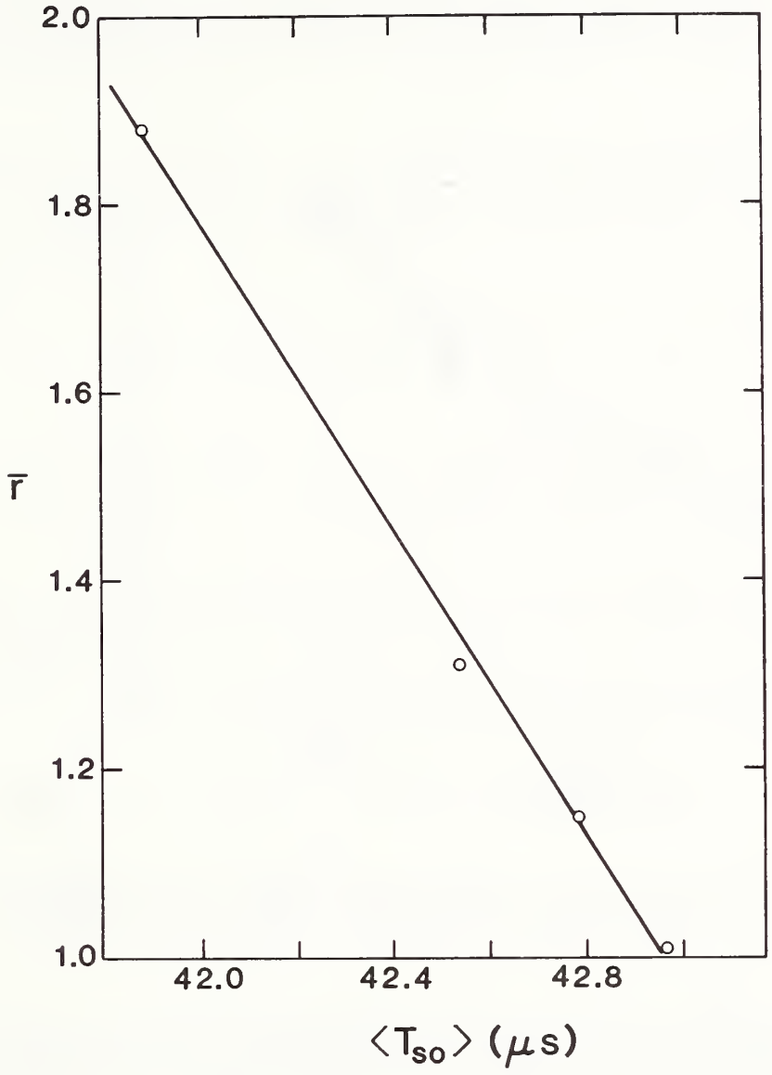

Figure 1. Relation between averaged arrival time of S_0-mode, $\langle T_{S0} \rangle$, and average r-value, $\bar{r}$.

When the resulting ultrasonic values of $\bar{E}$ are plotted versus $\bar{r}$, the results are as shown in Figure 2. Here the solid line represents the best fit to the data of Reference 1 and the open circles represent the S_0-mode data. These data are within the scatter band of the data of Reference 1. This indicates that the ultrasonic technique gives results comparable to the modul-r technique currently in use.

Consequently, an EMAT-based acoustical array, propagating S_0-mode waves at 0°, 90°, and 45° could be placed at a small liftoff above sheet to characterize formability on-line. As a first step in technology transfer an EMAT system

has been constructed whose signal-to-noise ratio on thin ferritic steel sheet is comparable to conventional (piezoelectric) transducers. As currently configured, this system consists of a single transmit-receiver EMAT pair, which measures arrival times (with EMATs in situ) with a precision of 1 ns or better when 100 arrival times are measured and averaged. At the current pulse repetition rate, the system reads out an averaged arrival time about once a second. One possible application for an array would be in the press-shop, where blanks having unacceptable formability could be rejected before proceeding through the production line. Another application would be on-line in a steel rolling mill.

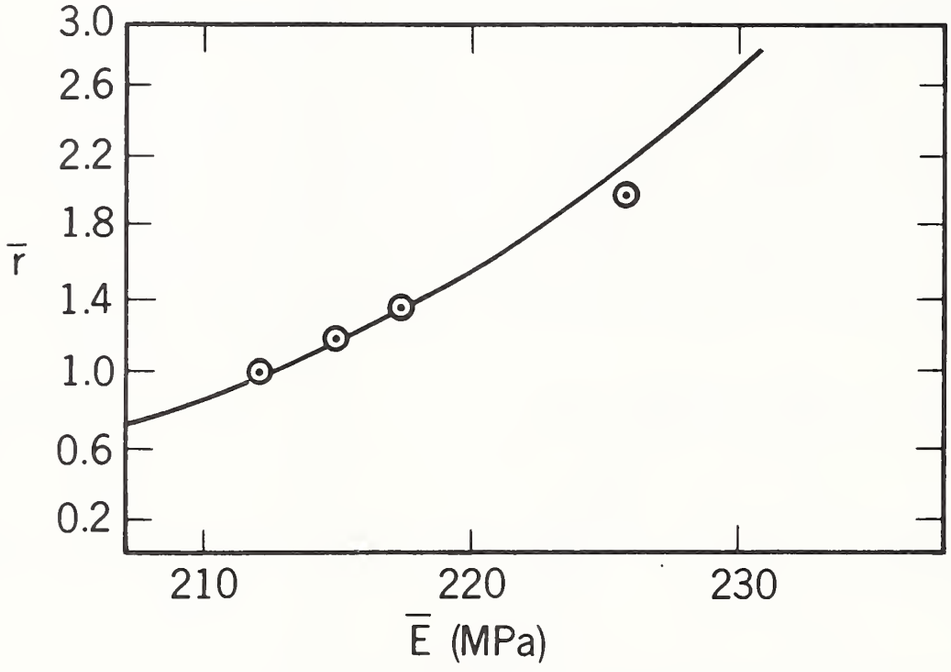

Figure 2. Comparison of correlation of $\bar{r}$ with $\bar{E}$ made with EMATs (open circles) and correlation made with experimental setup of Reference 1 (solid line).

In addition, the NIST participants in this program are now collaborating with researchers in the Advanced Steel Processing and Products Research Center (ASPPRC), a joint government-business-academia consortium involved in research to produce better sheet, bar, and plate stock. The prototype EMAT system described above was demonstrated to representatives of steel and automotive companies in the Center and received a favorable reception. It was decided, as part of this collaboration, that a larger data base would be obtained by measuring $\bar{r}$ both ultrasonically and by destructive means. A number of sheets covering a large range of $\bar{r}$ will be supplied by Center members who will measure $\bar{r}$ destructively. These will then be compared with nondestructive values obtained ultrasonically.

If the correlation for this larger data base appears good, NIST researchers will explore various means of technology transfer. These include guest workers who will learn EMAT-based measurement technology and give guidance on how

systems need to be configured for production environments; possible development of improved prototype systems which could be demonstrated in pilot projects at participating ASPPRC laboratories.

References:

1. C. A. Stickels and P. R. Mould, "The Use of Young's Modulus for Predicting the Plastic-Strain Ratio of Low-Carbon Sheet Steels," Met. Trans. 1, pp. 1302–1312 (1970).

2. A. V. Clark, R. C. Reno, R. B. Thompson, J. F. Smith, G. V. Blessing, P. P. Delsanto, and R. B. Mignogna, "Texture Monitoring in Aluminum Alloys: A Comparison of Ultrasonic and Neutron Diffraction Measurement," Ultrasonics 26, pp. 189–197 (1988).

3. A. V. Clark, Jr., "Ultrasonic Characterization of Texture and Formability," MRS Bulletin XIII, pp. 40–42 (1988).

4. A. V. Clark, G. V. Blessing, R. B. Thompson, and J. F. Smith, "Ultrasonic Methods of Texture Monitoring for Characterization of Formability of Rolled Aluminum Sheet," Rev. of Prog. in Quant. NDE 7B, pp. 1365–1373 (1988).

5. R. C. Reno, R. J. Fields, and A. V. Clark, "Crystallographic Texture in Rolled Aluminum Plates: Neutron Pole Figure Measurements," Rev. of Prog. in Quant. NDE 7B, pp. 1439–1445 (1988).

Ultrasonic Evaluation of Metal Surface Finishes

G. V. Blessing and D. G. Eitzen
Automated Production Technology Division
Center for Manufacturing Engineering

The measurement of surface finish is important in many areas of manufacturing. Sensor development for on-line monitoring of a material's surface condition is, therefore, of much interest for controlling automated manufacturing processes. In order to provide such a sensing capability, we have been applying noncontacting ultrasonic scattering and reflection techniques utilizing the machining coolant stream to couple the ultrasonic signal to the part. This technique provides for the evaluation of both average surface roughness and detailed surface profilometry on parts in situ during the manufacturing process.[1,2]

In the last years' reports we presented results on the application of an ultrasonic sensor to monitor the surfaces of rapidly rotating cylindrical parts (e.g., during machining at a turning center) and to scan the surfaces of flat and curved stationary parts (e.g., during machining at a milling center). In both of these applications the ultrasonic probe produced an area-averaging beam. In this report we present results obtained using a finely focused ultrasonic beam to map the topography of a surface in a fashion analogous to the (contacting) stylus profilometry technique.

The potential of the ultrasonic sensor as a profilometer was evaluated using 30 MHz focused ultrasound on a precisely shaped sinusoidal aluminum surface with a unidirectional lay. The average surface roughness R_a was 1.0 μm, and the surface periodicity Λ was 800 μm.[3] Both echo-amplitude and transit-time measurements were made, traversing perpendicular to the surface lay at a focal distance of 2 cm with the specimen immersed in water. The echo-amplitude data provided a measure of Λ, while the transit-time data provided a measure of local surface height.

Figure 1 compares the results of a contacting stylus scan[3] with an ultrasonic echo-amplitude scan perpendicular to the lay on the sinusoidal specimen. It is important to note that the received echo signal is a convolution of the incident beam dimension, the surface topography, and the transducer. For example, the echo amplitude signature in Figure 1(b) by itself provides no surface height information. The transducer used here was a broadband (highly damped) spherically focused element of diameter 6 mm, focal length 20 mm, and a half-amplitude beam width of 200 μm in the focal region.

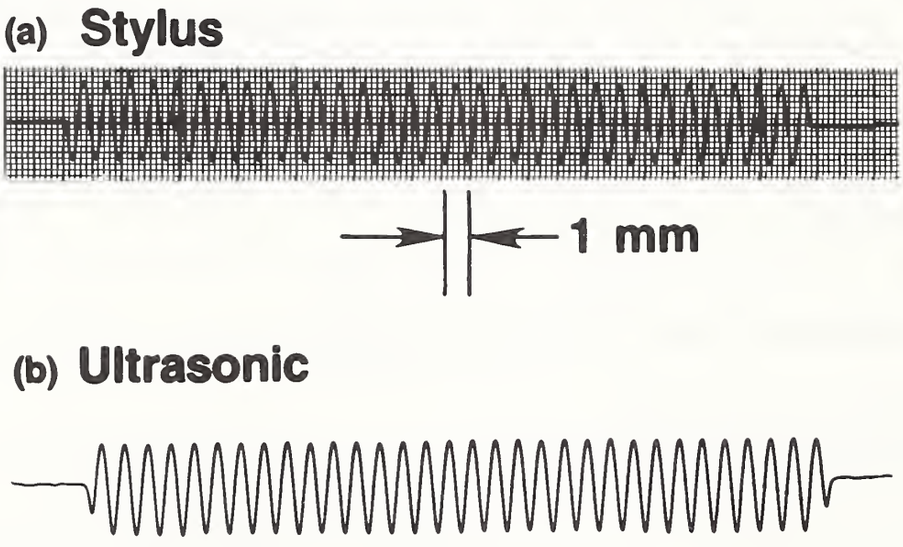

Figure 1. Profilometry scans of a 1.0 μm R_a sinusoidal aluminum surface by (a) a contacting stylus, and (b) a noncontacting ultrasonic echo-amplitude technique.

In contrast with the ultrasonic amplitude scan of Figure 1(b), Figure 2 is a transit-time scan of the sinusoidal surface. Discrete measurements of relative transit time for the round-trip distance between transducer and surface were taken at 100 μm steps perpendicular to the lay. A sinusoidal pattern of periodicity 0.8 mm is readily observed. (The negative slope superposed on the sinusoidal pattern is an artifact caused by the changing temperature of the water coupling medium during the scan.) Compensating for the slope artifact, and knowing the sound speed in water at room temperature (1.49 mm/μs), a nominal surface peak-to-valley distance of 2.5 μm was calculated from the data of Figure 2. However, the correct peak-to-valley dimension of the 1.0 μm R_a surface is π μm. This discrepancy is attributed principally to the finite beam

width of the incident ultrasound. The effect of beam width, which was nominally 25 percent of the surface periodicity in this case, was to average surface feature distances, thereby reducing the apparent peak-to-valley dimensions. For these surface and beam dimensions, a deconvolution of the data (based on the beam width) would be required for an accurate measurement of surface height.

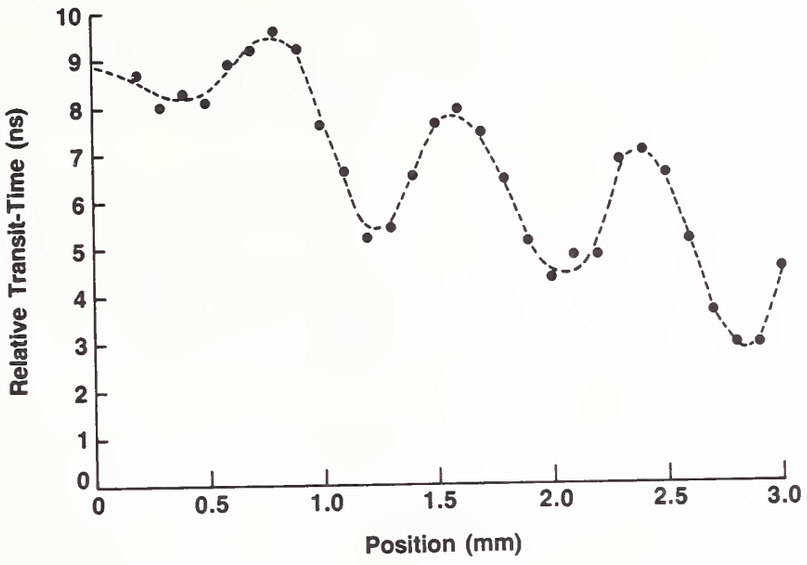

Figure 2. Profilometry scan of the same surface scanned in Figure 1 using an ultrasonic transit-time echo technique.

Future plans include increasing the ultrasonic frequency to profile finer dimensions, studying ground surfaces and perhaps the grinding wheel itself, and measuring specific surface features by means of ultrasonic surface waves that would follow the surface contour details.

References:

1. G. V. Blessing and D. G. Eitzen, "Surface Roughness Sensed by Ultrasound," to be published in Proceedings of Metrology and Properties of Engineering Surfaces International Conference held at NIST, 13-15 April 1988.

2. D. G. Eitzen and G. V. Blessing, "Ultrasonic NDE for Surface Roughness," MRS Bulletin XIII, No. 4, pp. 49-52 (April 1988).

3. G. V. Blessing and D. G. Eitzen, "Ultrasonic Real-Time Monitoring Device for Part Surface Topography and Tool Condition In Situ," U.S. Patent No. 4,738,139 (issued 19 Apr 1988).

III. NDE FOR COMPOSITES PROCESSING AND INTERFACES

The goal of this activity is to develop generic approaches, sensors, and procedures for quantitative NDE of composites and interfaces. As in the two previous activities, the emphasis is on measurements that can be made during the manufacturing process to sense the properties of the product during critical stages of its formation and to provide the data required to control the process to optimize quality and productivity. Since the knowledge base on composites characterization is far from complete, we expect that a portion of this activity will be concerned with relating important composite characteristics with performance and then developing NDE monitoring methods.

This activity includes research on utilizing fluorescent spectroscopy to monitor the processing of polymer matrix composites; applying ultrasonic techniques to improve the understanding and ability to monitor interfaces; and utilizing photothermal radiometry (thermal wave NDE) to monitor the quality of ceramic coatings on metals. Noteworthy accomplishments in this activity include:

- A major barrier to the implementation of advanced polymer composite materials in many applications is that the processing lacks the desired reliability. To improve the reliability, nondestructive evaluation measurement techniques need to be developed to improve process monitoring and control. Last year's research showed that fluorescence spectroscopy appeared to be feasible to monitor the non-Newtonian shear viscosity of polymer melts during processing. This year's research extends the technique's application to the monitoring of polymer molecular orientation, velocity, and flow characteristics. These parameters play a key role in determining the properties of composites.

- The characterization of interfaces is of vital importance in designing and manufacturing advanced composites. Theoretical and experimental research over the last two years has shown that ultrasonic waves radiate a fraction of their energy into the surrounding matrix, in the form of leaky ultrasonic waves, as they propagate along a fiber. Research this year experimentally confirmed the quantitative aspects of the model for iron/aluminum and silicon carbide/aluminum metal matrix composites.

Measurement and Control of Polymer Processing Parameters Using Fluorescence Spectroscopy

A. J. Bur, F. W. Wang, and A. Lee
Polymers Division
Institute for Materials Science and Engineering

The need for improved monitoring of polymer processing has escalated in recent years because of the large demand and market for advanced polymer materials that require tight controls on processing conditions over a broad range of variables. To satisfy these new requirements, we are developing sensors based on fluorescence spectroscopy to monitor process conditions on-line at the molecular and microscopic level.[1,2] The objective of our program is to utilize

these new measurement techniques in conjunction with processing models to predict and control the materials properties and performance of the final product.

Work during FY88 has focused on four areas: the design of experiments to measure fluorescence anisotropy and non-Newtonian viscosity as a function of shear rate; the chemical synthesis of a polymeric chromophore that is being used in experiments to measure fluorescence anisotropy; the development of a mathematical model to describe fluorescence photobleaching recovery and its relationship to velocity and flow characteristics; and negotiation with industrial laboratories for the purpose of carrying out collaborative research and development programs on polymer processing problems of mutual interest.

Fluorescence Anisotropy and Synthesis of a Polymeric Chromophore:

Fluorescence anisotropy measurements are being carried out using a capillary flow apparatus and a Weissenberg rheometer. The capillary flow apparatus is used in conjunction with a commercial fluorimeter so that fluorescence and viscosity can be measured simultaneously. A capillary is positioned vertically in the sample chamber of the fluorimeter and the shear rate experienced by the specimen is controlled by adjusting the pressure applied at the top of the capillary. We recently completed optical instrumentation of the Weissenberg rheometer and we are using it to carry out fluorescence and rheological measurements. The range of shear rates covered by these instruments is approximately 10^{-2} to 10^{2} s^{-1}

Fluorescence anisotropy measurements are being conducted on a low molecular weight polybutadiene specimen doped with a polymeric chromophore. The polymeric chromophore, which was synthesized in our laboratory, consists of polybutadiene tagged with fluorescently active anthracene so that the anthracene is situated at the center of the polymer chain. Infrared and gel permeation chromatography verify that anthracene has been placed in the central position and that the resultant number average molecular weight is approximately 12,000, as expected.

Our working hypothesis for the anisotropy experiments is that, for a non-Newtonian fluid, the fluorescence anisotropy increases (and the viscosity decreases) with increasing shear rate, and that the underlying cause of this effect is molecular orientation. The fluorescence anisotropy experiment is designed to measure this molecular orientation. In our first experiments we tested the converse of this hypothesis, i.e., for a Newtonian fluid fluorescence anisotropy is independent (as is the viscosity) of shear rate. Low molecular weight polybutadiene, M_n = 2800, which was doped with the tagged polybutadiene (10^{-4} molar concentration), was observed to be Newtonian and to have constant anisotropy in the shear rate range 1 to 100 s^{-1}. We conclude that, within the sensitivity of our measurement, molecular orientation of the tagged polybutadiene does not occur. Experiments using non-Newtonian polybutadiene, M_w = 22,000, are now in progress.

Velocity and Flow Characteristics:

A sensor to measure velocity, velocity gradient, and wall slip near the wall of a processing machine was designed and a mathematical model to describe its behavior was formulated. The sensor operation is based on fluorescence photobleaching recovery (see Figure 1). The design consists of an optical fiber that is fitted through the wall of a processing machine and is flush with the inside wall. Polymeric material, which contains a photobleachable dye, flows past the end of the optical fiber and the fluorescence properties in a defined region at the end of the fiber are observed. At a given instant, the dye in the probed volume is photobleached by a short pulse of ultraviolet radiation. As a function of time, fluorescently active material flows into the probed volume and the detected fluorescence intensity increases. In the model, we analyze this fluorescence recovery and derive a functional form for intensity versus time. From the equations, it is possible to distinguish between laminar flow and wall slip and, in the case of laminar flow, to obtain values for velocity and velocity gradient. Experiments to test this model will be carried out in FY89.

Interactions with the Polymer Processing Industry:

Considerable effort was exerted in order to increase the amount of industrial interaction and participation in our polymer processing program. A news release, which was issued from the NIST Public Relations Division, generated over thirty responses from major polymer processing companies. We responded to each request and are in active negotiation with a half dozen companies concerning the establishment of research associateships. The contacts that were developed via the news release were invited to participate in the NIST Intelligent Processing of Materials Workshop, August 31, 1988.

References:

1. A. J. Bur, F. W. Wang, and R. E. Lowry," Fluorescence Monitoring of Polymer Processing: Mixing and Zero Shear Viscosity," Proc. Soc. Plastics Eng., Annual Tech. meeting, April 1988.

2. F. W. Wang, A. J. Bur, R. E. Lowry, and B. M. Fanconi, "Fluorescence Monitoring of Polymer Processing," Polymer Materials Science and Engineering 59 (1988).

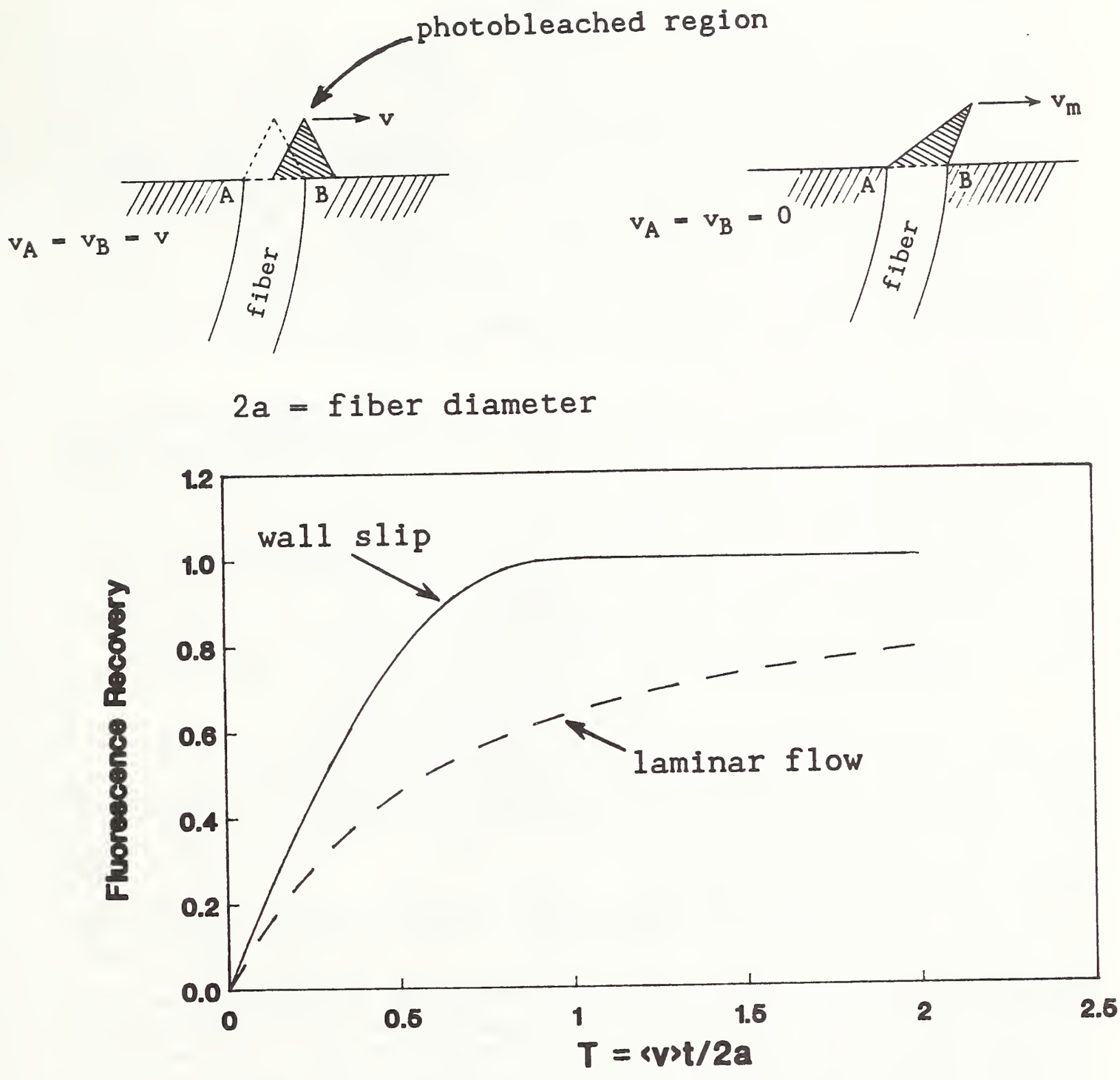

Figure 1. The principle of operation of the velocity sensor is fluorescence recovery after photobleaching. The shaded region at the end of the optical fiber is a photobleached region of a flowing material, whose movement is monitored by the fluorescence recovery. The results of a model calculation of the fluorescence recovery are plotted as a function of reduced time T. For equal average velocities <v>, recovery for wall slip is much faster than for laminar flow.

Guided Interface Waves

H. N. G. Wadley, J. A. Simmons, and E. Drescher-Krasicka
Metallurgy Division
Institute for Materials Science and Engineering

Research this year has focused on using leaky ultrasonic waves to interrogate physically inaccessible interfaces of metal matrix composite (MMC) fibers. Our research exploited our earlier discovery of elastic waves that radiate a fraction of their energy into the surrounding matrix as they propagate along a fiber.[1] Progress has required a close coupling of experimental and theoretical work. The general quantitative description of modes in composites was reported[1] and the specific equations describing leaky waves in MMC without an interface zone have been carefully analyzed.[2] The results of these calculations indicate four families of waves in a single fiber composite. A direct linkage has also been established between these families and the rod modes of the fiber. The existence of leaky waves from two of the branches has been experimentally confirmed in Fe/Al and SiC/Al MMC during this year's research.

In experiments on the Fe/Al system, surface type rod modes were used for generation and detection of interface waves. For the experiments, a surface acoustic wave was transmitted along a steel rod (the model fiber); see Figure 1. After passing into the aluminum matrix, this mode converted to a combination of leaky modes. The receiving transducer was placed at different points of the matrix and the acoustic response was measured. The resultant signal was decomposed into its component modes, identified by their peaks, to permit comparison with the theory. All modes whose leakage angles permitted measurements were detected. We have drawn a practical conclusion from these experiments: the modes with low leakage angle and low attenuation are convenient for measuring the average velocity along a fiber; those with higher leakage angle are more convenient for local velocity measurements along the fibers..

Studies were also conducted on the SiC/Al system using an SiC rod. Some of the modes, which arise from a different type of rod than that used in the Fe/Al specimens, were experimentally confirmed. This part of the research was partially done in cooperation with Professor B. T. Khuri Yakub of Stanford University. A scanning system was built in order to increase the applicability of ultrasonic interface waves to a direct interface characterization. The schematic diagram of the experiment is shown in Figure 1. A movable conical transducer, later changed to a monofrequency pinducer, was placed against the outer surface of the composite SiC/Al sample. The receiver was moved along the specimen surface while the transmitter excited an interface wave that propagated along the interface. The phase velocities of different leaky modes were measured directly by monitoring the changes of the receiver positions $\Delta x = x_2 - x_1$ and related changes of the travel time $\Delta t = t_2 - t_1$. The results, the phase velocity of interface leaky wave $v_I = \Delta x/\Delta t$, were compared with the calculated dispersion curves for each particular SiC/Al interface mode. Figure 2 draws the calculated dispersion curve together with the experimental results for one of these modes. The dotted lines on this figure show the attenuation of this mode.

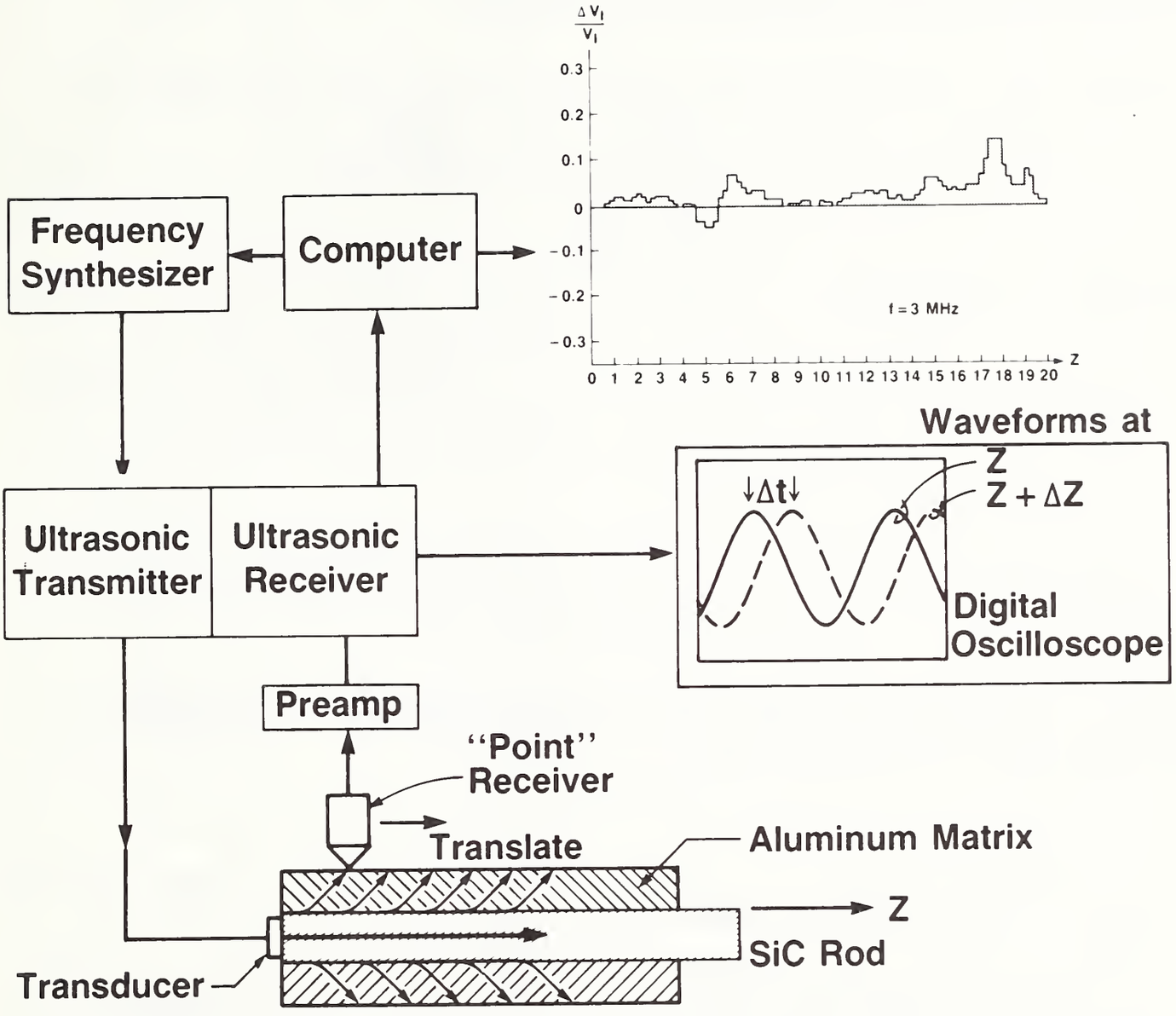

Figure 1. The schematic diagram of the ultrasonic measurements on SiC/Al interfaces.

It is worth noting that the maximum phase velocity of this mode of 18564 m/sec represents the fastest ultrasonic wave ever measured. This velocity is about twice that of the longitudinal velocity in SiC and about three times that of the longitudinal velocity in aluminum. While infinite velocities are theoretically possible for rod modes near their cutoff frequencies, we are not aware of any technique that permits the experimental observation of these rod waves modes at high phase velocity.

This mode was also used in our approach to measure the local variations in velocity over a section of SiC/Al interface. Changes in the velocity of MMC

interface waves are expected to be related, through inverse techniques, to the changes in the elastic moduli near the interface.

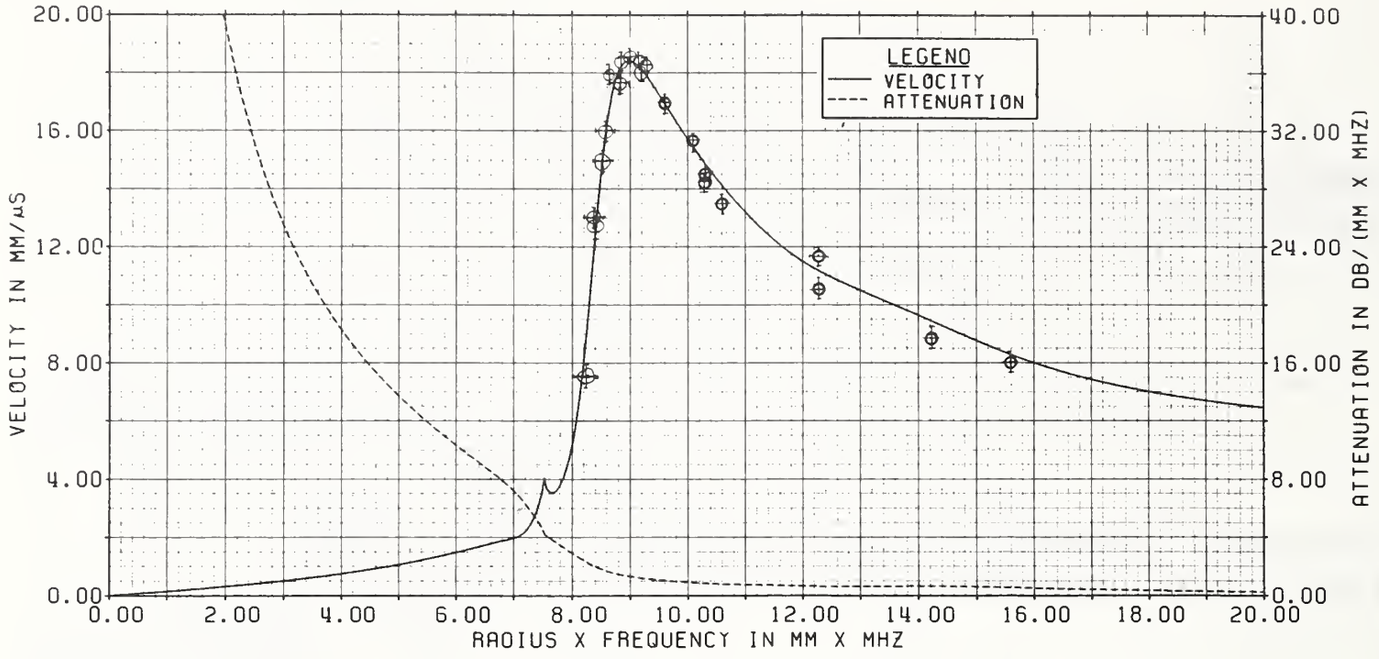

Figure 2. Comparison between calculated (continuous line) and measured (points) dispersion curve for SiC/Al interface leaky mode. The dotted line shows the calculated attenuation.

References:

1. E. Drescher-Krasicka, J. A. Simmons, and H. N. G. Wadley, "Guided Interface Waves," Rev. of Prog. in QNDE 6B, pp. 1129-1136 (1987).

2. H. N. G. Wadley, J. A. Simmons, R. B. Clough, F. Biancaniello, E. Drescher-Krasicka, M. Rosen, T. Hsieh, and K. Hirshman, "Composite Materials Interface Characterization," 1st Progress Report for SDIO, NBSIR 87-3630, March 1988.

Thermal Properties of Dielectric Films Using Thermal Wave Techniques

H. Frederikse, X. T. Ying,* and A. Feldman
Ceramics Division
Institute for Materials Science and Engineering

*Guest Scientist from Fudan University, Shanghai,
Peoples Republic of China

The purpose of this project is to inspect the thermal behavior and mechanical integrity of non-metallic coatings using the propagation of thermal waves. Such coatings play an important role in many technological areas: optical

components, engines and combusters, corrosion protection, electronic devices, etc. Thermal wave techniques have gained considerable attention and popularity during the last 10 to 12 years. Especially thin and thick layers, from a few microns to several millimeters, can be probed conveniently by thermal waves because the thermal diffusivity length can be adjusted to these depths by varying the modulation frequency. Several detection schemes can be used to determine the temperature variations in time or in space; a number of these techniques do not require contact with the material being probed and, hence, lend themselves well for nondestructive evaluation.

Last year we developed photothermal radiometry (PTR) as a noncontact method to monitor the thermal quality of ceramic coatings at room temperature. During the present reporting period we have investigated the heat resistance of a number of oxides at elevated temperatures up to 900 °C. The oxide coatings, deposited by plasma spraying to a thickness of 50 to 100 μm, were chromia, zirconia, and alumina; the substrates were stainless steel plates in all cases. This work was done in collaboration with Grady White of the Ceramics Division who is also doing thermal wave research (see report on page 32).

The experimental set up is pretty much the same as that described in last year's report. The only difference is that the sample is positioned inside a horizontal cylindrical furnace, some 6 to 8 cm from the opening at one end. Measurements were made at six temperatures between 20 and 900 °C. Two infrared detectors were employed over this temperature range: a liquid nitrogen cooled InSb detector for temperatures up to 500 °C and a germanium photodiode for temperatures between 500 and 900 °C. This change of detectors was dictated by the fact that the InSb detector saturates above 500 °C due to the d.c. thermal signal. Even in the range of 200 to 500 °C small apertures had to be inserted to limit the amount of radiation falling on the sensitive InSb area. Similar considerations applied to the Ge photodiode.

At every temperature the magnitude of the signal, $|S|$, and the relative phase, $\Delta\phi$, were measured as a function of the modulation frequency from 9 to 30 Hz. Analysis of the $\Delta\phi$-vs-$\sqrt{f}$ plot yielded the desired results for the thermal diffusivity α and the thermal conductivity κ of the coatings. The values of α and κ are about a factor two smaller than the handbook data for bulk specimens (and <u>much</u> smaller than the single crystal values). This is not surprising considering the high degree of disorder and the relatively low density of plasma sprayed coatings. Another indication of the large scatter is the temperature dependence; α and κ show a nearly constant behavior rather than the predicted 1/T dependence.

In the last few months we have turned our attention to the thermal properties of diamond films. Since about two years ago there has been a sudden surge in interest in diamond coatings produced by chemical vapor deposition or sputtering techniques. NIST has launched a program in this area including both preparation and characterization. One of the properties of great importance is the high thermal conductivity of diamond. Consequently it is important to determine this property both as a guide for applications and as a measure of the quality of the diamond films. In recent months we have studied several thermal wave techniques in order to determine the most suitable method for

diamond coatings. Results have been obtained on a 1/2-mm-thick film (obtained from GE). In this case PTR was the preferred method. Other promising approaches are the longitudinal method, propagation of the heat wave along a film of diamond deposited on a narrow strip of thermally insulating ceramic, or a variation of the optical beam deflection technique (mirage effect).

Plans for FY 1989 are focused on the diamond films and the appropriate thermal wave techniques for their evaluation.

IV. NDE STANDARDS AND METHODS

The objective of the Standards and Methods activity in the NDE Program is to provide the scientific understanding of NDE measurement methods and to develop, maintain, and disseminate effective standards for NDE measurements that are traceable to national standards.

Five project reports from the NDE Standards and Methods activity are presented this year dealing with ultrasonics and acoustic emission, eddy currents, magnetic methods (primarily Barkhausen), real-time radiology, and the capacitance array sensor. Two of these reports cover two of the largest efforts in the NDE Program but all five of the reports document significant progress. It is fair to say that the NDE Standards and Methods activity is the cornerstone of the entire NDE Program, as it continues to serve as the basis for intensive standardization and consultation services provided to the nation's NDE community.

The reduction in the number of reports presented this year (there were nine last year) is due, in part, to retirements by some of the NDE Program's senior researchers. Thus, for example, the Program's long-term project on standards for film radiography was terminated following Robert Placious' retirement. However, ONDE's continuing interest in radiation methods is apparent in the new project on real-time radiology (or radioscopy) that was started a year ago. This redirection reflects ONDE's ongoing effort to anticipate the NDE community's changing needs for standards as technology advances.

Elsewhere, the recent retirement of Julius Cohen brought a halt (hopefully temporary) to the Program's project on thermographic NDE. It is intended to resume the project next year with replacement talent. Similarly, progress in the Program's leak testing project had to be put on hold this year due to staffing problems in the Center for Basic Standards. This important work will also be resumed next year.

Despite these interruptions, productivity in the NDE Standards and Methods activity in fiscal year 1988 was good. A few brief examples of this year's accomplishments follow:

- Thomas Siewert of the Fracture and Deformation Division and Leonard Mordfin of the Office of Nondestructive Evaluation negotiated an agreement with representatives of the Army Materials Technology Laboratory (MTL) and the General Electric Aircraft Engines Quality Technology Center for a joint effort to develop document standards (military and ASTM) on real-time x-ray radioscopy (RTR) for nondestructive evaluation. Under the terms of the agreement GE will develop drafts on the basis of their company standards and MTL will provide funding to NIST to incorporate measurement considerations into the documentary standards. As a corollary benefit to NIST, Siewert has been granted access to MTL's and GE's RTR laboratory facilities for research purposes. GE's facilities in Cincinnati, in particular, are among the most advanced in the country.

- A new "Standard Test Method for Minimum Detectable Temperature Difference for Thermal Imaging Systems," which was developed in the NDE Program, is proceeding through the ASTM balloting process. This document represents the second of three test methods that will define the critical performance parameters of thermographic NDE instruments. (The first standard, on minimum resolvable temperature difference, was adopted by ASTM last year.)

- ONDE's long-term contract from the MTL to develop new and improved military standards for NDE was especially fruitful this year. A standard fieldworthy method for verifying the performance of acoustic emission (AE) testing systems is described in MIL-HDBK-786, prepared by Donald Eitzen of the Center for Manufacturing Engineering (CME). A key feature of the method is the simulated AE event developed earlier by Nelson Hsu of CME and for which he received an IR-100 award. Standard glossaries of terms and definitions for ultrasonic testing procedures and for radiographic testing were prepared by Eitzen and by E. H. Eisenhower of the Center for Radiation Research and were issued as Military Standards 371 and 369, respectively.

- ASTM has initiated work on the development of a new standard test method to assess the visual acuity of inspectors and others who read and interpret radiographs. The basis of the standard is a set of 72 reference radiographs of artifacts containing tight discontinuities (artificial cracks) in different locations, orientations, contrasts, etc. The set was developed by Robert Placious of the Center for Radiation Research, following a scheme conceived earlier by Gary Yonemura, formerly of the Center for Building Technology. This development was accomplished in the NDE Program with partial support from the MTL. Although intended originally for radiographic applications, it is now anticipated that the new test method will also prove useful to practitioners of other NDE disciplines, such as visual inspection and liquid penetrant testing, where visual acuity is a critical factor.

Magnetic Methods and Standards for NDE

L. J. Swartzendruber
Metallurgy Division
Institute for Materials Science and Engineering

A variety of magnetic methods are currently used in nondestructive evaluation, both for detecting defects and for verifying material properties. Some of these methods, such as magnetic particle inspection, magnetic flux leakage testing, and magnetic permeability measurement, are widely used in industry; the first two for defect detection, and the latter for property determinations such as ferrite content in stainless steel welds. A number of methods (Barkhausen noise, magnetoacoustic emission, magnetomechanical damping, and ac magnetometry) have been used on a limited scale but require further development to increase their reliability and make them more widely applicable. Finally, some magnetic property measurements (e.g., saturation magnetization, coercivity, and initial permeability) contain a wealth of information concerning

material properties that have barely begun to be exploited. Effort on this project during the year has been primarily directed to Barkhausen noise analysis.

Progress:

Many workers have shown that measured properties of Barkhausen noise can be related to material properties such as hardness, grain size, internal stress, and defect density. When usable, the Barkhausen method is very attractive because high production rates are possible. However, the relationship between the observed noise and a material property is always heuristic and is generally poorly understood from a fundamental point of view; this could lead to erroneous conclusions.

There are many ways to characterize Barkhausen noise, including (1) the noise pulse amplitude distribution profile, (2) the power spectral density, (3) the pulse number spectrum, and (4) the total noise power. Commercially available equipment uses one or another of these methods to produce a "Barkhausen number" that changes when a material property changes. The same method does not appear to be used by any two pieces of equipment. Our purpose has been to develop an experimental arrangement that will have the flexibility to calculate these "numbers" from the characteristics of the observed noise as well as to allow a detailed analysis of the noise from a fundamental point of view. This will be accomplished primarily by software analysis of digitized noise signals.

The experimental arrangement is illustrated in Figure 1. A computer is used to control a high speed, dual channel digitizing oscilloscope, a frequency synthesizer, and a bipolar power supply. The bipolar power supply is used to energize a yoke which swings the sample through a hysteresis loop with a frequency and amplitude controlled by the synthesizer. An offset current from the power supply can be set by the computer in order to trace out minor loops on the hysteresis curve of the sample. Two pickup coils are placed on the sample; an encircling coil A and a pancake coil B. Both coils can be used to observe Barkhausen noise. In addition, coil A can be used to measure the total flux density in the sample, thereby tracing out the hysteresis loop of the sample. The noise from one or both pickup coils is amplified by a preamplifier and then digitized by the oscilloscope. The digitized information is transferred to the computer via an IEEE-488 bus. By using direct memory access, transfer rates up to 400 kbaud can be realized.

With the loop being traced at a frequency of 0.1 Hz, a complete noise spectrum in the frequency range 0 to 25 kHz can be transferred to the computer for a single loop in 10 seconds, with the total amount of information being 500 kilobytes. This noise frequency range is adequate for almost all applications. (Much higher noise frequency ranges, up to about 1 MHz, could be used with the present equipment but much longer times would be required for obtaining and analyzing the data.) Much of the basic software required to operate the equipment and analyze the noise has been developed and installed with the aid of a guest worker from Israel. This guest worker is also attempting some fundamental modeling of the elementary Barkhausen jumps.

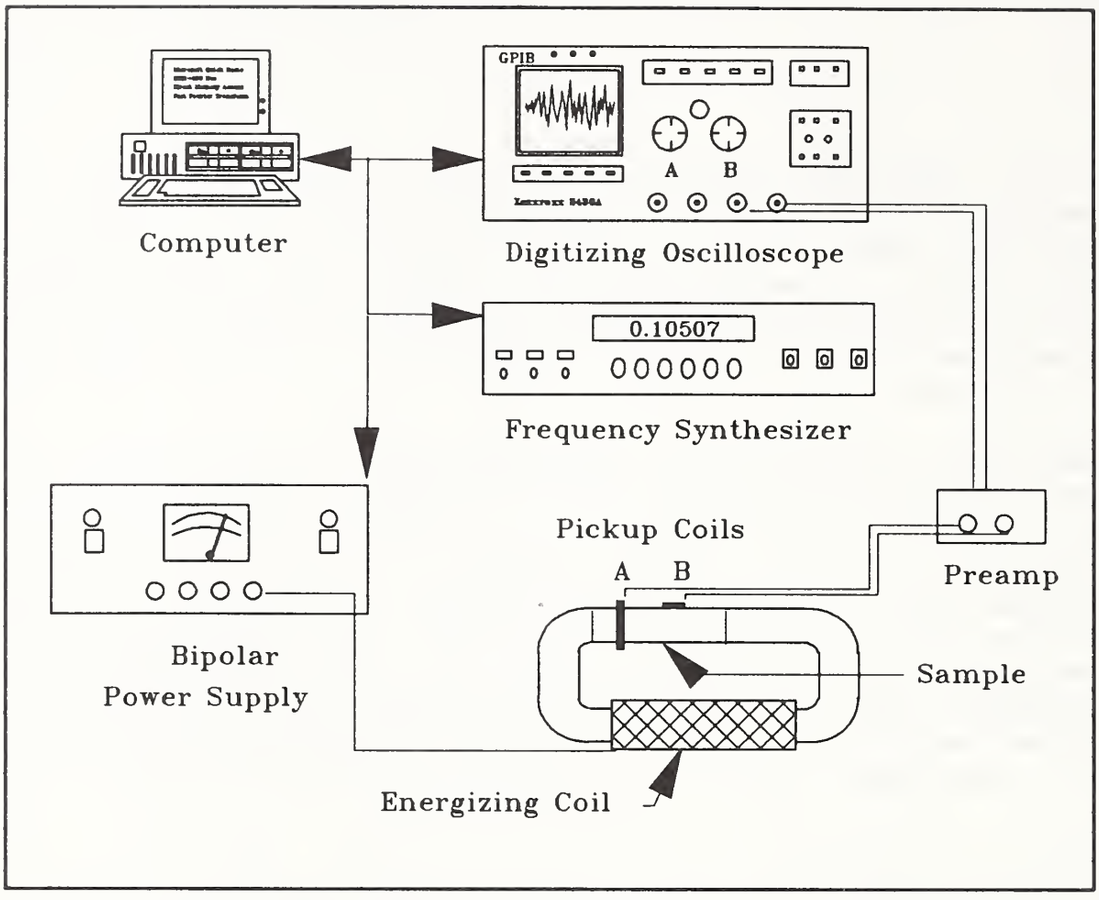

Figure 1. Experimental system for detailed analysis of Barkhausen noise characteristics.

A second version of the military standard for magnetic particle inspection (MIL-STD-1949) was prepared and coordinated (work supported by the U.S. Army Materials Technology Laboratory). Valuable comments were obtained from over fifty companies. We also are participating in conversion of this standard to an ASTM document. As part of this work, a round robin on the use of standard artificial flaw shims in magnetic particle inspection was conducted. The response to this round robin was inadequate to establish the validity of the use of these standard shims. The poor response is believed due to the large effort required by participants in the round robin. Important as these standards are, most organizations are simply too busy inspecting to put forth the required effort. A new round robin is being planned that will provide more limited, though useful, results with much less effort on the part of the participants.

Effort during the coming year will focus on further development of our Barkhausen system and associated software and on obtaining and analyzing Barkhausen noise from selected steels with a variety of microstructures. The goal will be to develop materials with very well characterized noise properties that can be used as standards to compare the outputs from different types of noise analyzers. As an important part of this effort, optimization of the

pickup coil-preamplifier combination will be pursued with the aid of a new guest worker.

Eddy Current Methods and Standards

T. E. Capobianco and F. R. Fickett
Electromagnetic Technology Division
Center for Electronics and Electrical Engineering

Coil Construction-Factor Study:

Because of the statistical analysis requirements of empirical modeling, the coil construction-factor study described in our last report has undergone substantial modification this year. The study has been redesigned to allow use of modern statistical design techniques and to account for the scatter winding of commercial coils. The initial study design complicated the statistical analysis of potential interactions between construction factors, and the selection of coils was not based on statistical principles which allow us to optimize the amount of information from a minimum number of data points.

The new design, developed with the help of the Center for Applied Mathematics, is based on the statistical concept of multi-dimensional response surface modeling and uses sophisticated software which can place design points so as to produce the most information with the fewest number of points. In our case, each design point in the study is a coil to be wound, so efficiency of experimental design is a major consideration. One of the appealing features of this new design is that placement of the design points is independent of the criteria to be optimized. Thus, response surfaces can be determined for inspections on high or low conductivity alloys, and for different crack geometries using a single coil set.

For such empirical statistical models it is desirable to have an overdetermined data set. For the six factors (listed in Table 1) varied at three levels each (ferrite diameter is at two levels) 40 to 50 coils would be both an achievable number to wind and an adequately overdetermined set.

The additional factor of coil repeatability, or homogeneity of the set, is also a concern. The coil set determined using the statistical design software has 40 different constructions to be wound, with 10 repeats at selected points to provide a measure of the winding homogeneity, for a total of 50 coils. Additional ferrite cores were needed to build this set. Unfortunately, the desired shapes and sizes are not commonly available over the entire range of permeabilities necessary for our study and, thus, the lead time for manufacturing the ferrites turned out to be over ten weeks. Also, at the beginning of the year we had expected that another 12 to 15 coils, in addition to the 18 finished last year,[1] would yield a complete set on which an empirical model could be based. Instead, we're facing the task of winding 50 new coils in a completely redesigned experiment. Therefore, construction of the model relating coil fabrication to inspection sensitivity will not be completed until next year. The coils already constructed will enable us to evaluate relative

sensitivities of the precisely layered coils compared to similar scatter-wound coils in the new set.

Table 1. Construction Factors

Factor	Levels
Ferrite diameter (mm)	0.89, 1.40
Number of turns	90, 120, 180
Winding distance from end (mm)	0.38, 0.76, 1.14
Ferrite permeability	800, 1500, 6500
Aspect ratio	0.5, 1.0, 2.0
Wire gauge (AWG)	40, 44, 48

Next year this newly designed study will result in a sound empirical model that will allow us to move on to the next logical extension of this work, namely a manufacturability study which implements this model in a production environment and enlists the participation of commercial probe manufacturers.

Stanford Delta Z Program:

Provisions for the NIST installation of the Stanford/ONDE developed eddy current ΔZ calculation computer program have been completed. A contract was arranged with the program's author, Steve Jefferies. Mr. Jefferies visited NIST-Boulder in August and installation, preliminary checkout, and training were completed. The program will assist in modeling and evaluation of coil geometries and flaw interactions.

Artifact Standards:

We are exploring a new technique for producing eddy current artifact standards that involves tightly closed artificial discontinuities of an exactly known size. Although this work was not a part of the proposed plan this year, the idea evolved as a result of interactions on our probe characterization standard and the accompanying round robin.[2] The initial results look promising and, if subsequent work confirms our expectations, we intend to pursue a patent on the technique. Some of these results were presented at the QNDE conference in August,[3] and further refinement of the technique is now in progress. If the preliminary results are proved correct, we envision using these artifacts in conjunction with a "standard probe" and offering the set as a probe and system characterization package.

NDE Application of SQUIDs:

As a result of interest generated by our presentation at the Navy SQUID NDE Workshop,[4] we attempted a collaborative effort with Argonne National Laboratory to measure manufactured and actual defects in nuclear reactor heat exchanger tubing using an ASTM specified artifact. Our approach was to keep the apparatus as simple as possible since this was to be an exploratory study. We used the SQUID in an unshielded arrangement with a pair of superconducting coils configured as a first order gradiometer as the input. Our hope was that this type of input would partially compensate for running unshielded. The coils were adjacent and coplanar and wound in series opposition. This gradiometer was mounted in a fiberglass-epoxy tube which was fitted with a pair of copper saddle coils that provided a field normal to the gradiometer coils. The tube was made to fit inside the ASTM sample and to look for defects from the inside wall. Unfortunately, the electrical noise in our lab is severe and the SQUID was barely able to maintain lock. This indicated the need for extensive shielding, or perhaps higher order gradiometer coils. Neither arrangement could be realized in the actual environment anticipated for these tests. We suggested that more conventional magnetic NDE techniques would be more appropriate for this application.

Two Axis Positioner and Data Acquisition System:

This year we purchased, with Division funds, an AT-class computer as the foundation of a sophisticated eddy current data acquisition system utilizing a two axis positioning apparatus and our existing impedance analyzer. This system represents a major change in direction regarding both hardware and software. In the past we have relied on a borrowed positioning system, but when the coil parameter study grew to its present proportions, it became obvious that this system was no longer adequate.

The new system gives us significant advantages in mass storage, computational speed, and flexibility. Our software is being developed in Pascal, which offers the advantages of being faster and more powerful than BASIC and the code can be written with greater clarity. Using the serial interface, this computer controls a two axis positioner. The tables ride on recirculating ball bearings over the 46-cm (18 in) range of each axis and have a minimum step size of 0.013 mm (0.0005 in) and repeatability of $\pm$ 0.0013 mm (0.00005 in). Eddy current probes will be carried by a counterweighted, articulated, fiberglass-epoxy arm, which is presently under construction. Probe data from the impedance analyzer will be read into the computer over a GPIB-488 bus.

References:

1. T. E. Capobianco and D. F. Vecchia, "Coil Parameter Influence on Eddy Current Probe Sensitivity," Review of Progress in Quantitative NDE 7A, pp. 487-492 (Plenum, NY, 1988).

2. L. L. Dulcie and T. E. Capobianco, "New Standard Test Method for Eddy Current Probes," Proc. of the 36th DoD Conference on NDT, pp. 154-160 (U.S. Army Aviation Systems Command, St. Louis, MO, 1987).

3. T. E. Capobianco and J. C. Moulder, "Standard Flaws for Eddy Current Probe Characterization," Proc. of the Review of Progress in Quantitative NDE, La Jolla, CA, August 1-5, 1988.

4. F. R. Fickett, "Review of NBS Work in SQUID-Based NDE," SQUID/NDE Workshop, Harper's Ferry, WV, April 13-15, 1988.

Application of Capacitive Array Sensors to Processing of Ceramics and Composites

P. J. Shull and A. V. Clark
Fracture and Deformation Division
Institute for Materials Science and Engineering

B. A. Auld
Ginzton Laboratory
Stanford University

Capacitive array probes are attracting increased attention because of their potential for robotic sensors and for nondestructive evaluation, especially for cure monitoring of composites. In most applications, the probe is non-contacting and scans the workpiece; in composites, the probe is usually inserted inside the composite layup.

Here we report on two new applications of these sensors: noncontacting characterization of (a) sintering of ceramics and (b) curing of composites. Both applications depend upon the fact that the complex dielectric constant changes during material processing.

For noncontact applications, the probe impedance (or its reciprocal, the admittance) depends upon several factors: probe geometry, distance to specimen (liftoff), and the electrical properties of the specimen (dielectric constant, ϵ). Thus, it is necessary to have a theory that can be used to deduce ϵ from admittance measurements, in the presence of liftoff.

In general, the liftoff is unknown. In fact, even if the probe is placed on the workpiece, there will still be an unknown amount of liftoff due to effects such as protective covering over probe electrodes, nonuniform electrode thickness, etc. These effects, while seemingly small, can have an influence on admittance, especially for small probes with closely spaced electrodes. For example, we have found a liftoff of approximately 100 μm can cause a change in ΔY approaching 100 percent; the worst case we have measured. ΔY is the difference between the probe admittance in air, and the admittance in the presence of the specimen.

In our work on sintering of ceramics, we have constructed probes of different geometries and tested them on a variety of ceramics with different ϵ. Our initial idea was to multiplex the electrodes to vary the probe's electrical geometry, and use an elementary theory to predict both ϵ and liftoff, d, from our admittance measurements. One problem with this theory is illustrated in

Figure 1, where we show ΔY versus d for a material having a relative dielectric constant of 50. The theory (curve A) predicts a monotonic decrease of ΔY with liftoff whereas the measurement (curve D) shows a sharp drop followed by a recovery. Similar results were obtained on other ceramics.

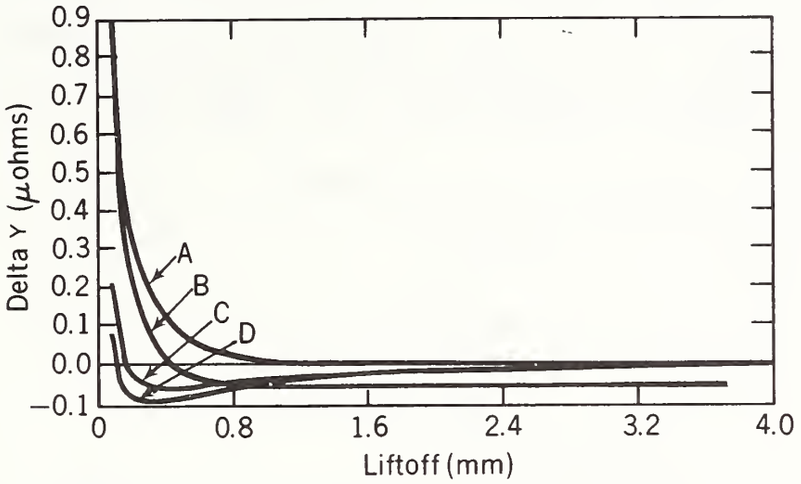

Figure 1. Liftoff response for different probe geometries and boundary conditions: A – theoretical, B – 2-D probe to reduce edge effects, C – miniaturized probe with ground plane approximately 100 mm from the specimen, D – miniaturized probe with specimen on the ground plane.

We have identified several causes of the discrepancy between theory and experiment. The elementary theory requires that the probe have a sinusoidally varying potential which averages to zero. We have found that our impedance measuring instrument creates a probe potential field that has both a spatially-varying component and a constant component. We refer to these as the non-zero and zero spatial frequency components, respectively. The potential fields created by these components are calculated by the finite element method and shown in Figure 2. Figure 2a shows the resultant potential field from the sinusoidally-varying component of the electrode configuration. This indicates very little interaction with the ground plane. In contrast the potential field of the constant component, Figure 2b, is greatly distorted by the presence of a ground plane. We have made measurements which show that the capacitance to ground for the constant component is about ten times the capacitance predicted if the probe were part of a parallel plate capacitor with the same area.

We are developing techniques to suppress these measurement artifacts. Increasing the distance between electrodes having opposite polarity (decreasing spatial frequency) is a partial solution, as is increasing the distance between specimen and conductors in the environment. The latter effect is shown in Figure 1, curve C, where the specimen is 100 mm from a ground plane. Further suppression of the "recovery" occurs when the electrodes are designed to reduce charge concentration and when they are mounted on a low ϵ substrate. See Figure 1, curve B.

We have also made experiments to demonstrate proof-of-concept of noninvasive cure monitoring of composites. Here a major concern (for graphite-epoxy composites) is the shielding that occurs due to specimen conductivity. (This

is not a concern for probes embedded in the composite). For example, we have monitored the cure of a thin plate of commercial ("5 minute") epoxy that was placed on one side of a 6-mm thick panel of unidirectional graphite-epoxy; our probe was placed on the opposite side. Results of our experiment are shown in Figure 3. We found that the magnitude of the impedance changes dramatically with curing. The percentage change is larger at 1 kHz than at 100 kHz. The phase angle, while close to −90° (indicating primarily a capacitive coupling between probe electrodes), does show a change due to conductivity of the epoxy. The percent change is again higher for 1 kHz than for 100 kHz.

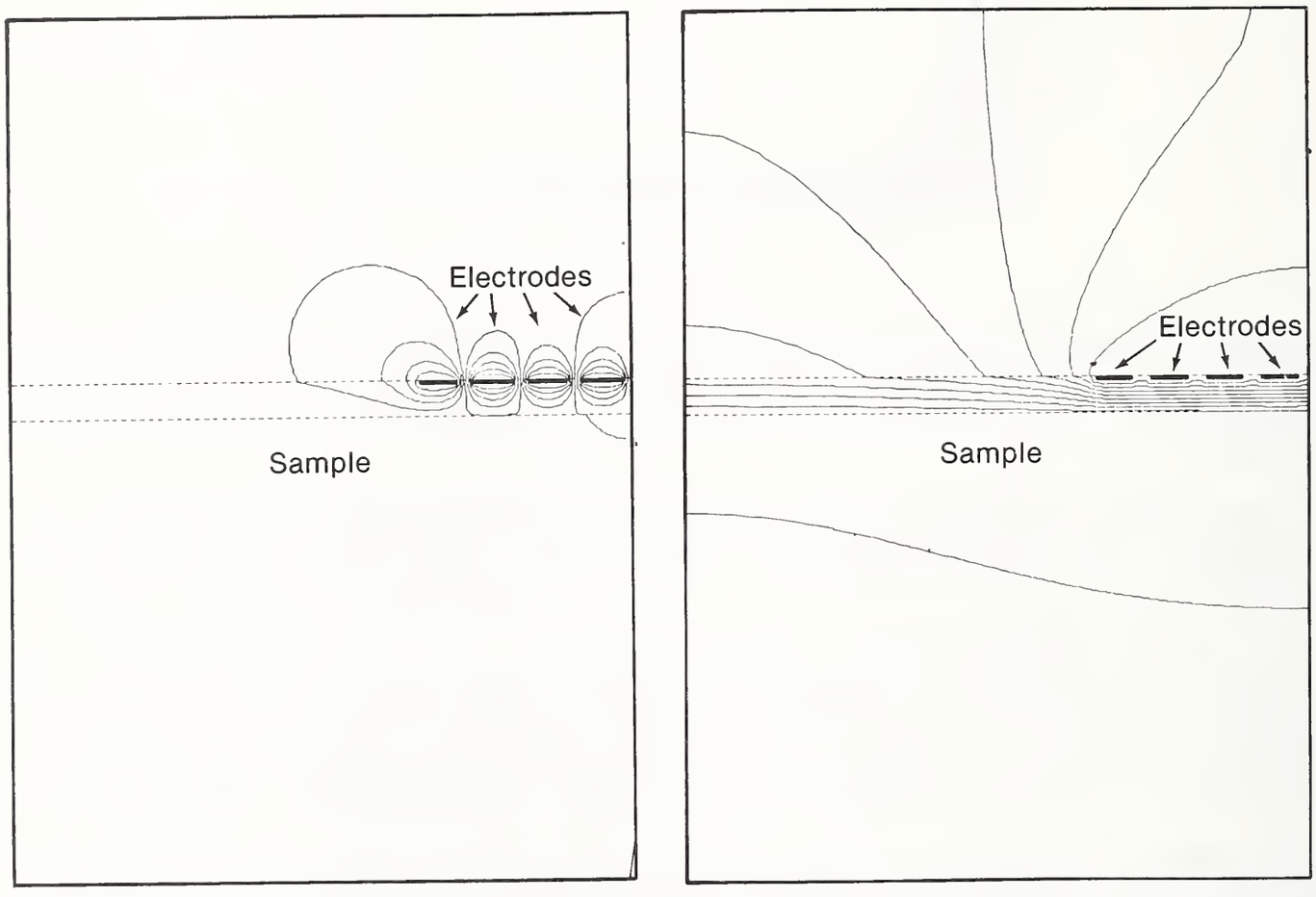

(a) (b)

Figure 2. Finite-element calculation of the potential field showing the probe-sample-environment interaction - (a) the non-zero spatial frequency component and (b) the zero spatial frequency component.

We have developed a mathematical model of the interaction of the probe's electrostatic field (in air) with the electrodynamic field in the conducting composite. The resulting equations are being developed into a finite element code that will be used to calculate the field in the composite and also the probe admittance, as the dielectric constant and conductivity vary during cure. This will give insight into means of extracting information about the state of cure in thick composites. The depth to which the electrodynamic

field penetrates can be varied by changing either probe geometry or the frequency of probe excitation.

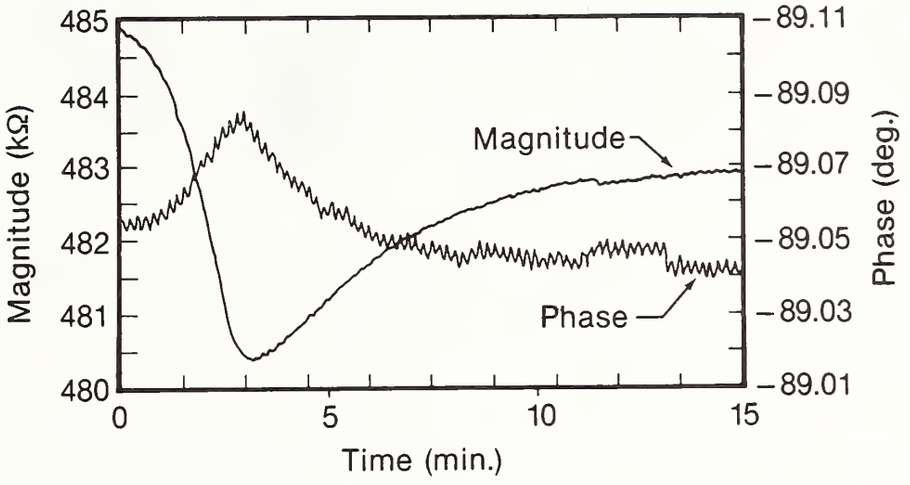

Figure 3. Probe response--impedance magnitude and phase vs. time--to a curing epoxy with a 6-mm thick conductive material (graphite-epoxy composite) place between the probe and the epoxy.

NDE Standards and Methods: Ultrasonics and Acoustic Emission

D. G. Eitzen and the Ultrasonic Standards Group
Automated Production Technology Division
Center for Manufacturing Engineering

The objective of this project is to develop and disseminate artifact and documentary standards, develop and maintain measurement and calibration services, and develop new or improved methods for acoustic emission and ultrasonic NDE techniques. The documentary standards are typically guided through ASTM and then promoted as international standards. The calibration services for acoustic NDE methods are essential to the NDE community and referenced around the world.

Our transducer development work is motivated by the need for devices to transfer calibrations to sensor users/suppliers and for precision dynamic motion measurement for new or advanced acoustic methods. The development of new ultrasonic and AE methods also relies heavily on theoretical analysis to gain a better understanding and new insight into the physics of the sound-structure interactions that lead to the development of new generic methods or adaptations for specific applications.

Our documentary standards activities in the last year were again very productive. With partial support from the Army MTL, two new MIL documents were published; MIL-STD-371,[1] an ultrasonics glossary, and MIL-HDBK-786,[2] an AE system field assurance guide using the Hsu pencil source for producing simulated AE. An article on "AE Sensors and Their Calibration" was published as

a chapter in the ASNT handbook on acoustic emission testing.[3] The article provides user information on AE sensors and disseminates information on primary calibration and on NIST-developed tools for secondary calibration. Standards activities through ASTM and ISO continue to grow. Data and techniques are being developed to revise four ASTM standards, and significant effort is directed at two new ISO standards. The chairmanship of ISO/TC 135/SC 3 continues to require significant effort. Also, responsibility (joint with ONDE) has been assumed for organizing a joint ASTM/NIST/ASNT symposium on NDE standards to be held in the fall of 1989.

Methods for secondary calibration of AE sensors are under development. The objective of this effort is to devise an inexpensive and convenient system for transferring the calibration of acoustic emission transducers. A priori, any system that would place a source transducer in face-to-face contact with the receiving transducer, has been rejected. It has been established that the mechanical impedance of a receiving transducer interacts significantly with that of the driving object on which it is mounted. The mechanical impedance of a transducer is likely to be a complicated function of frequency, and there is no known way to calculate or measure this impedance. Therefore, the interaction between the mechanical impedances of two transducers placed face to face would produce results that would be impossible to analyze.

The choice of a (calibration) block to be interposed between source and receiving transducers is dominated by the necessity that the propagation modes in the block be calculable and that the block have a mechanical impedance that matches that of the medium on which the transducer is to be used.

As a first attempt, a steel plate 3.3 cm thick by 90 cm square was tried as a calibration block. Elasticity theory predicts the transfer function for the plate, and experimental results using a capillary-break source and an NIST conical transducer receiver agree remarkably well with the theory. (See last year's report for this project, Figure 1.) Two alternative schemes were considered for the secondary calibration system. Both schemes use a source on the surface of the block, and two receivers equally spaced from the source. One of the receivers is the reference transducer (RT) and the other is the transducer under test (TUT). In one scheme, the source is a capillary break and the receivers feed transient recorders followed by Fourier analyzers. In the other scheme, the source is an NIST conical transducer driven by a tone burst. The receiver signals are gated to remove reflections and other unwanted signals, and the transfer function at each frequency is measured directly by means of a variable attenuator and detector. In both schemes, the transfer function obtained using the TUT is divided by that obtained using the RT, frequency by frequency.

Scheme 1 and scheme 2 were both tried on the 3.3-cm-steel plate using a TUT having a wear face diameter of approximately 1.5 cm. Results of both tests (Figures 1, 2) can be compared with the normal calibration (Figure 3) for the TUT, and it can be seen that both schemes give poor results. However, if the large NIST calibration block is substituted for the 3.3-cm-steel plate, then the results are in reasonable agreement with the normal calibration.

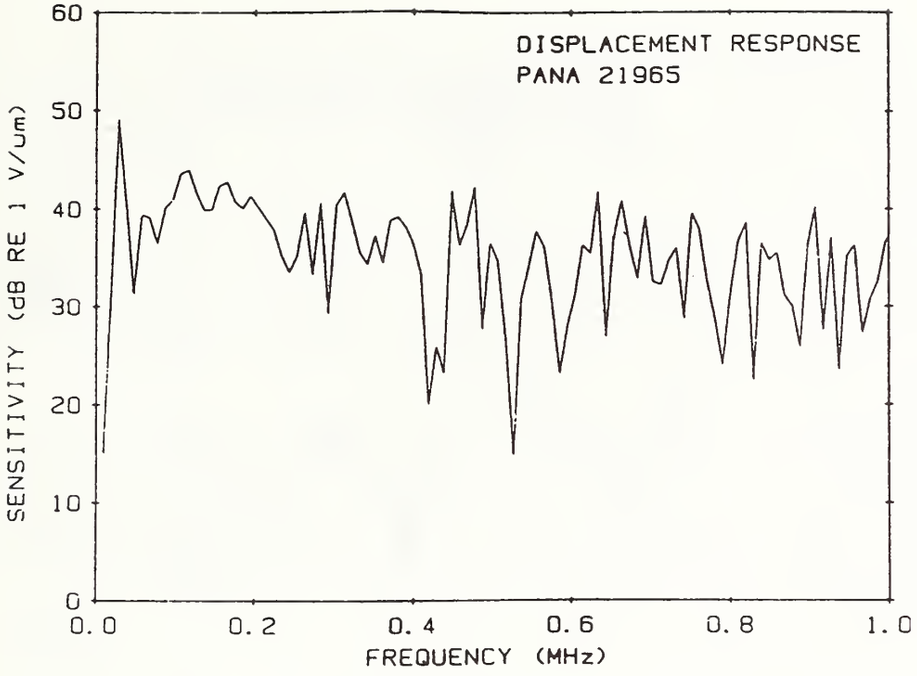

Figure 1. Test of secondary calibration performed according to scheme 1 on a 1.5-cm diameter AE transducer using a 3.3 cm thick by 90 cm square steel plate as the transfer block. The reference transducer was an NIST SRM 1856 conical transducer; the source, a glass capillary break.

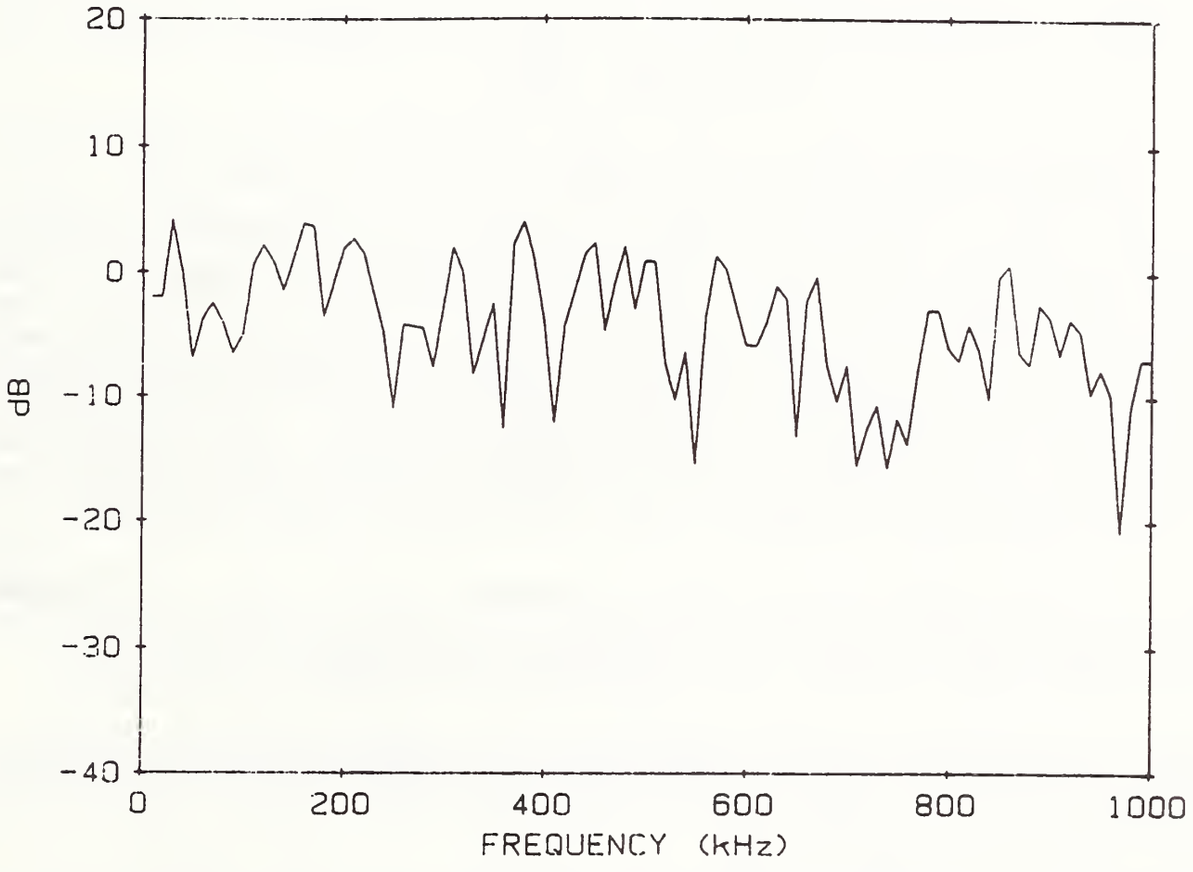

Figure 2. Test performed on 3.3 cm by 90 cm square steel plate similar to scheme 2. The source was an NIST conical transducer, and the transducer under test was the 1.5-cm diameter AE transducer.

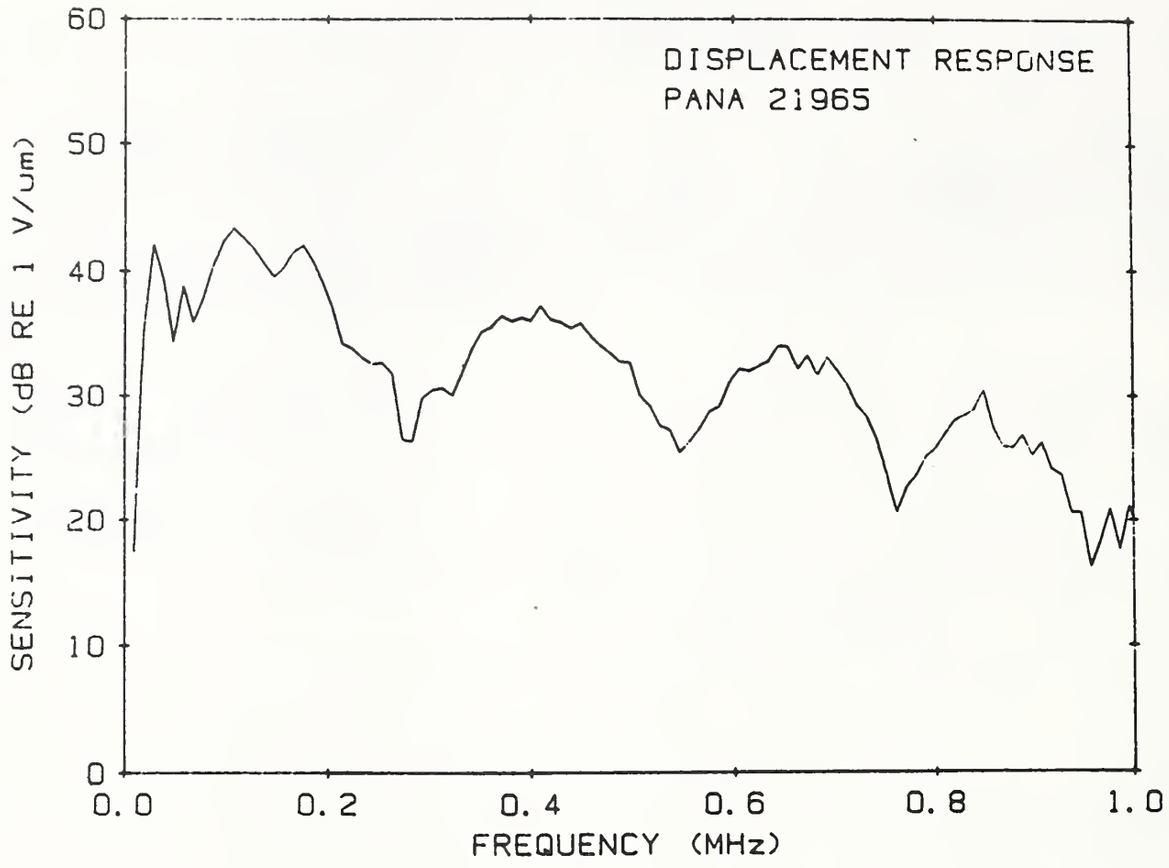

Figure 3. Primary calibration of the 1.5-cm diameter AE transducer.

The explanation for the failure of the 3.3-cm plate as a calibration block lies in the complicated interaction between the motion of the surface of the plate and the aperture effect of the transducer. The fact that a point transducer, such as the NIST conical transducer, produces a correct waveform for the plate indicates that point transducers could be calibrated on the plate, but the extended transducer does not calibrate correctly. The features of the plate waveforms resulting from a step function force source vary markedly with distance from the source and travel with different speeds. The aperture effect of the transducer is different for each feature of the waveform.

The results obtained using the extended transducer on the steel plate impugn all experiments in which extended transducers are used to measure motion on plates. For meaningful results it is essential to use point transducers.

We believe that a steel block 20 cm thick by 40 cm square would be a good compromise; working time would be sacrificed, with attendant loss of low frequency accuracy, but the surface pulse waveforms would replicate those of the large block within the working time.

Simulated acoustic emission sources have been studied theoretically and experimentally. The interest is in enhanced tools for calibration and field tests, in tools for point impact/point receiver methods, and in tools to develop remote measurement techniques. Consider, for example, the ball impact

source. Hertzian theory provides the dynamic stresses for an elastic ball colliding with an elastic half space. Combining this theory with elastic plate theory, one can calculate displacements in a plate resulting from collision with a ball. The result is a source with reasonably known characteristics. Ball bearings between 1/16 inch and 3/8 inch have been dropped onto an 8.9-cm-thick glass plate from a height of 3 cm. An NIST conical transducer located on the bottom of the plate opposite the source was used to measure the dynamic normal displacement at that point. The transducer had been calibrated by a capillary-break experiment on the same plate.

The experimental waveforms from the dropping ball experiments were convolved with the inverse Green's function of the plate in an attempt to recover the source waveforms. Comparison of these source waveforms and those calculated from Hertzian theory shows some discrepancy that we attribute to the fact that it has not yet been possible to compensate completely for the transducer's transfer function. Resolving this discrepancy is an important goal of this effort.

We have also considered repetitive transient sources. Electronically triggered sources which act to apply mechanical transient forces are desirable for several reasons; signal averaging may be applied to increase signal-to-noise ratio and accuracy, and Fourier analysis can be applied to obtain transient waveforms without using a digital transient recorder.

A piezoelectric device which applies a static load to a surface and then suddenly removes that load (like the capillary break) has been designed but not yet built. In the design, a parabolic interface between steel and brass acts as an acoustic lens to focus a rarefaction wavefront onto the point of contact between the device and the driven object.

The tangential transducer, reported in 1986, has a patent pending and a detailed article describing it was submitted for publication.[4] Construction of replicates has begun in order to assure manufacturability and efficient technology transfer. Data are also being collected to demonstrate the agreement between the measured waveforms and theory and to depict the added AE information available.

References:

1. Anon., "Glossary of Terms and Definitions for Ultrasonic Testing Procedures," MIL-STD-371 (15 October 1987).

2. Anon., "Field Assurance of Acoustic Emission System Operation Using Simulated Acoustic Emission Events," MIL-HDBK-786 (1 October 1987).

3. D. G. Eitzen and F. R. Breckenridge, "Acoustic Emission Sensors and Their Calibration," Nondestructive Testing Handbook, 2nd edition, Vol. 5, Section 5, pp. 121-134 (ASNT, Columbus, OH, 1987).

4. Thomas M. Proctor, Jr., "A High Fidelity Piezoelectric Tangential Displacement Transducer for Acoustic Emission," submitted to J. of Acoustic Emission.

X-Ray Radiography

T. A. Siewert
Fracture and Deformation Division
Institute for Materials Science and Engineering

Image quality standards designed for conventional radiography are not adequate for real-time radioscopy systems, whose use is increasing. Development of new radiation transfer standards was the preeminent need determined in the 1987 workshop on real-time radioscopy; improved measurement of overall system performance also ranked high. By cataloguing the uses of these systems and designing appropriate standards (devices placed in the specimen location to measure such characteristics as contrast and resolution), this program is addressing these needs.

Questionnaire:

To obtain the data upon which an appropriate radiation transfer standard could be developed, a questionnaire was distributed to users and producers of real-time systems at the January 1988 meeting of the ASTM Committee on Radiology; it requested information on industrial usage of these systems. Chairmen of ASTM subcommittees involved with real-time systems helped design the questionnaire and will receive a summary of the responses. A preliminary assessment of the fifteen replies received to date reveals certain trends:

- The energy range reported for the real-time systems varied widely, but a histogram (Figure 1) of the replies shows a plateau between 100 and 150 kV. This plateau in energy indicates the range for an initial design, a transfer standard which would serve the majority of users.

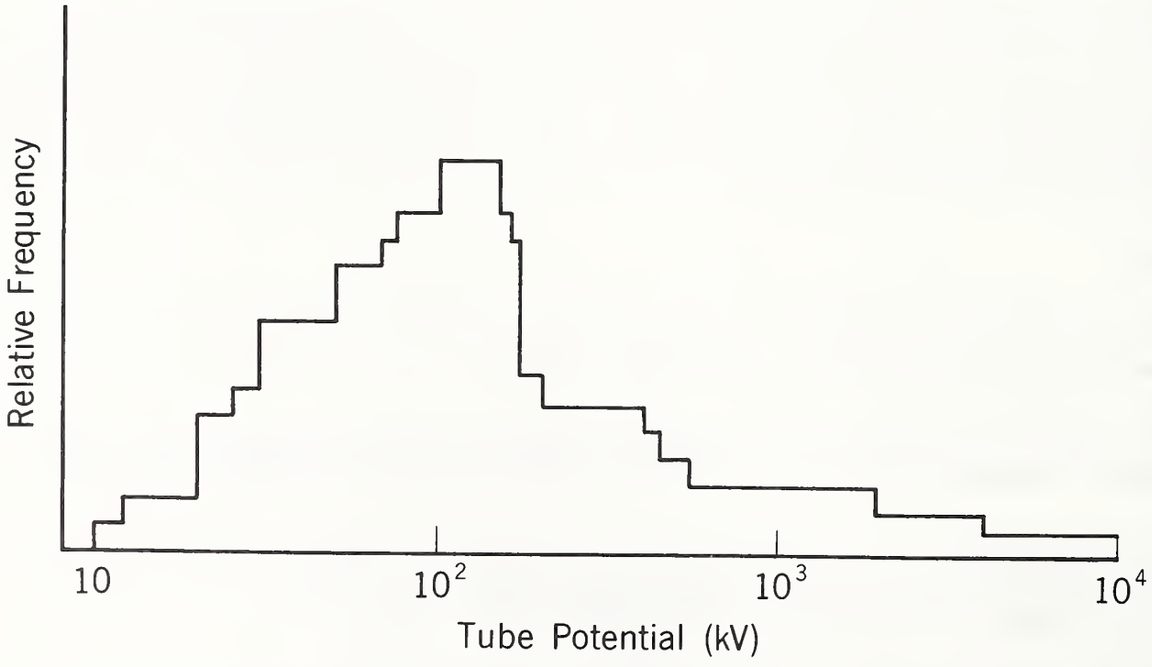

Figure 1. Histogram of potentials used in RTR systems.

- Aluminum was mentioned most often as a material examined by real-time systems. A histogram of the material thickness revealed a plateau near 10 mm; this correlates well with the penetrating capability of the plateau noted for system energy. Thus, a standard made of aluminum in this thickness range would satisfy the needs of most users.

- Steel was second in usage. Its histogram had a plateau between 6 and 30 mm. The 6-mm thickness could also be effectively penetrated by a 100 to 150 kV system. Polymer-matrix composites, silicon electronic circuit substrates, plastics, ceramics, titanium, and gold were also mentioned.

- A histogram was developed from responses to the resolution required by these systems; a plateau occurred between 2 and 10 line pairs per millimeter. This resolution range should be incorporated into the radiation transfer standard.

Replies to the questionnaire are expected from ASNT members who learned of our program at a July 1988 topical meeting on real-time radioscopy,[1] as well as the members of ASTM subcommittees. To obtain representative data for the spectrum of domestic usage, cooperation with additional industry and standards-making groups is being sought. A final report, which will be completed in late 1988, will describe the use of real-time radioscopy systems and form the basis for the design of a prototype standard.

New Image Quality Indicators:

New designs of image quality standards that will be fully compatible with the capabilities of real-time radioscopy systems are being developed. For example, conventional image quality indicators have been designed for the specimen oriented orthogonal to the beam, but real-time systems should accommodate rotation of the specimen.

The concept of an image quality standard with rotational symmetry has been developed; as the specimen rotates, image quality can be constantly measured. The initial concept includes spheres (with two degrees of rotational symmetry) or rods and cones (with one degree of rotational symmetry) that have a low-density core and a high-density coating. Figure 2 shows a cross section through one of these and its radiographic projection. Since the core is low-density material, it causes little attenuation of the beam, and the projection is primarily that of the coating.

The effective radiographic thickness of the central region is twice that of the coating. With proper choice of coating material and thickness, this region might function as a contrast standard. For thin coatings, the edge of the projection forms a sharp peak, which might be used to evaluate the modulation transfer function. The overall diameter of the projection provides a standard dimension for determining the magnification of microfocus units. For spherical shapes, the circular edge of the projection could reveal variations in width due to focal spot asymmetry, or it might be used to evaluate the effect of specimen movement during evaluation.

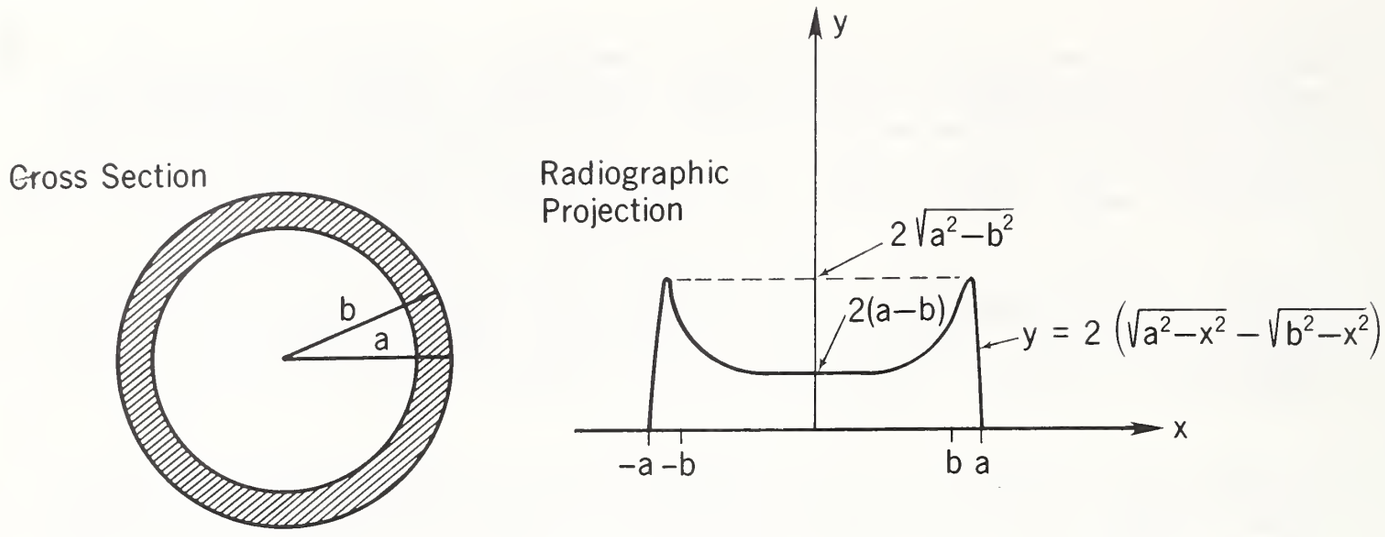

Figure 2. Cross section through a sphere or rod with low density core and a high density coating, and its radiographic projection.

Lucite spheres of 3-and 6-mm radius have been plated with copper to evaluate this concept. Coating thicknesses up to 0.03 mm have been achieved with electroless plating solutions; greater thicknesses have been achieved with subsequent electroplating. Preliminary radiographs show good edge definition at 60 kV. Evaluation of the other attributes is underway through cooperative programs with industrial laboratories.

References:

1. T. A. Siewert, "Standards for Real-Time Radiography – National Bureau of Standards," Paper Summaries, Real-Time Imaging III Topical Conference, pp. 21-24 (American Society for Nondestructive Testing, Columbus, OH, July 1988).

APPENDICES

APPENDICES

1. NDE SEMINARS AT NIST

Professor R. H. Cole, Brown University
"Dielectric Measurements of Material Properties"
November 9, 1987

NDE Poster Session
November 23, 1987

Professor Mack A. Breazeale, University of Tennessee
"Physics and Engineering Principles of Nonlinear Acoustics"
February 2, 1988

Professor Robert L. Thomas, Wayne State University
"Thermal Wave Imaging Using IR Video Techniques with Synchronous Heating"
May 27, 1988

Professor B. A. Auld, Stanford University
"Integrated Sensors for Robotics and Manufacturing Process Control"
June 10, 1988

2. INVITED TALKS BY ONDE STAFF

"Automated Materials Processing," H. T. Yolken, Welding and Testing Technology Conference, Knoxville, Tennessee, February 17, 1988.

"Nondestructive Evaluation of Monolithic Shipping Casks for Spent Nuclear Fuel," L. Mordfin, Lynchburg Section, American Society for Nondestructive Testing, Lynchburg, Virginia, February 17, 1988.

"Overview of the Nondestructive Evaluation Program at NBS," G. Birnbaum, Nondestructive Inspection/Evaluation Ad Hoc Working Group, Alexandria, Virginia, May 24, 1988.

"Intelligent Processing of Materials: A New Challenge for NDE," H. T. Yolken, Fall Conference, American Society for Nondestructive Testing, Anaheim, California, September 20, 1988.

"New Challenges for NDE," H. T. Yolken, Second Regional Congress for NDT for Latin America and the Caribbean, Lima, Peru, September 26, 1988.

3. PUBLICATIONS

Following is an incomplete listing of NIST reports and publications on NDE and related topics that have become available since last year's Technical Activities report was prepared.

Anon., "Glossary of Terms and Definitions for Ultrasonic Testing Procedures," MIL-STD-371, 11 pp. (15 October 1987).

Anon., "Field Assurance of Acoustic Emission System Operation Using Simulated Acoustic Emission Events," Military Standardization Handbook MIL-HDBK-786, 8 pp. (1 October 1987).

Anon., "Glossary of Terms and Definitions for Radiographic Testing," MIL-STD-369, 46 pp. (15 October 1987).

Anon., Six NBS Projects Win 1987 I-R 100 Awards," NBS Research Reports, NBS SP 735, pp. 20-22 (Dec. 1987).

T. C. Bagg, "Digitizing Documents: Guidelines for Image Quality," Inform 1, No. 11, pp. 6-9 (Nov. 1987).

G. Barnea and C. E. Dick, "Monte Carlo Studies of X-ray Scattering in Transmission Diagnostic Radiology," Medical Physics 13, No. 4, pp. 490-495 (Jul/Aug 1987).

M. A. Baum, "Back to the Basics," NBS Research Reports, NBS SP 735, pp. 5-8 (Dec. 1987).

G. Birnbaum, "NBS NDE Program," Proc. 16th Symposium on Nondestructive Evaluation, pp. xliii-xlv (Southwest Research Institute, 1987).

G. Birnbaum, "NBS Presentation," Summary Record of the 1988 Meeting of the Ad Hoc Working Group on Nondestructive Evaluation (NDE), Office of Science and Technology Policy (OSTP)/Committee on Materials (COMAT), IDA Memorandum Report M-474, pp. 21-37 (Institute for Defense Analyses, Alexandria, VA, July 1988).

G. V. Blessing and D. G. Eitzen, "Ultrasonic Real-Time Monitoring Device for Part Surface Topography and Tool Condition In Situ," U.S. Patent No. 4,738,131, 7 pp. (April 19, 1988).

G. V. Blessing, D. G. Eitzen, J. F. Henning, A. V. Clark, Jr., and R. E. Schramm, "Precision Ultrasonic Thickness Measurements of Thin Steel Disks," Review of Progress in Quantitative Nondestructive Evaluation 7B, pp. 1563-1572 (1988).

G. V. Blessing and M. P. Jones, "Characterization of Ceramics by Ultrasonics," Advanced Ceramics '87 Conference Papers (Society of Manufacturing Engineers, 1987).

T. E. Capobianco and F. R. Fickett, "A Proposed Military Standard for Commercial Eddy Current Probes Based on Characterization of Performance," Proc. 35th Defense Conference on Nondestructive Testing, pp. 134-141 (Ogden Air Logistics Center, UT, 1986).

T. E. Capobianco and D. F. Vecchia, "Coil Parameter Influence on Eddy Current Probe Sensitivity," Review of Progress in Quantitative Nondestructive Evaluation 7A, pp. 487-492 (1988).

D. Chandler-Horowitz and G. A. Candela, "Ellipsometric Instrumentation for Optical Metrology in Thin Films," Proc. SEMICON/West '87, pp. 126-132 (1987).

A. V. Clark, Jr., "Ultrasonic Characterization of Texture and Formability," MRS Bulletin XIII, No. 4, pp. 40-42 (Materials Research Society, 1988).

A. V. Clark, G. V. Blessing, R. B. Thompson, and J. F. Smith, "Ultrasonic Methods of Texture Monitoring for Characterization of Formability of Rolled Aluminum Sheet," Review of Progress in Quantitative Nondestructive Evaluation 7B, pp. 1365-1373 (1988).

A. V. Clark, J. C. Moulder, R. B. Mignogna, and P. P. DelSanto, "Comparison of Several Ultrasonic Techniques for Absolute Stress Determination in the Presence of Texture," Proc. ONR Symposium on Solid Mechanics Research for QNDE, Evanston, IL, Sept. 18-20, 1985, pp. 345-360 (1987).

A. V. Clark, R. C. Reno, R. B. Thompson, J. F. Smith, G. V. Blessing, P. P. Delsanto, and R. B. Mignogna, "Texture Monitoring in Aluminum Alloys: A Comparison of Ultrasonic and Neutron Diffraction Measurement," Ultrasonics 26, pp. 189-197 (1988).

R. B. Clough, H. N. G. Wadley, and R. Mehrabian, "Acoustic Emission Studies of Electron Beam Surface Modification of Aluminum," Metallurgical Transactions B 19B, pp. 493-503 (June 1988).

G. T. Davis, "Piezoelectric Polymer Transducers," Advances in Dental Research 1, No. 1, pp. 45-40 (Oct. 1987).

P. P. Delsanto, R. B. Mignogna, and A. V. Clark, Jr., "Ultrasonic Texture Analysis for Polycrystalline Aggregates of Cubic Materials Displaying Orthotropic Symmetry," Nondestructive Characterization of Materials II, pp. 535-543 (Plenum, 1987).

R. C. Dobbyn, M. Kuriyama, S. Takagi, and L. C. Chow, "High Resolution Radiography: Applications to Biomedical Imaging," Proc. Sixth Southern Biomedical Engineering Conference, pp. 194-197 (1987).

L. L. Dulcie and T. E. Capobianco, "New Standard Test Method for Eddy Current Probes," Proc. 36th Defense Conference on Nondestructive Testing, pp. 154-160 (U.S. Army Aviation Systems Command, St. Louis, MO, 1987).

K. C. Duvall, "Development of a Standard 2.5-MeV Neutron Source," Nuclear Instruments and Methods in Physics Research B24/25, pp. 893-896 (1987).

C. M. Eisenhauer, R. B. Schwartz, and R. C. McCall, "Effect of Air Scatter on Calibration of Instruments for Detecting Neutrons," Radiation Protection Dosimetry 19, No. 2, pp. 77-84 (1987).

D. G. Eitzen and G. V. Blessing, "Ultrasonic NDE for Surface Roughness," MRS Bulletin XIII, No. 4, pp. 49-52 (Apr. 1988).

D. G. Eitzen and F. R. Breckenridge "Acoustic Emission Sensors and Their Calibration," Nondestructive Testing Handbook, 2nd edition, Vol. 5, pp. 121-134 (ASNT, 1987).

B. M. Fanconi, F. W. Wang, and D. L. Hunston, "Comparisons Among Process Monitoring Techniques," Proc. 45th SPE Annual Technical Conference and Exhibit, pp. 1100-1102 (1987).

R. A. Forman, J. R. Hill, M. I. Bell, G. S. White, S. W. Freiman, and W. Ford, "Strain Patterns in Gallium Arsenide Wafers: Origins and Effects," Proc. Intl. Symp. on Defect Recognition and Image Processing In III-V Compounds (DRIP 1987), E. R. Weber, editor, pp. 63-71 (Elsevier, 1987).

H. Frederikse and A. Feldman, "Thermal Wave Inspection of Heat Resistant Ceramic Coatings," Nondestructive Testing of High-Performance Ceramics, pp. 177-182 (American Ceramic Society, 1987).

J. L. Gross, F. Y. Yokel, R. N. Wright, A. H. Fanney, J. H. Smith, G. E. Hicho, and T. R. Shives, "Investigation into the Ashland Oil Storage Tank Collapse on January 2, 1988," NBSIR 88-3792, 204 pp. (June 1988).

G. Harman, "Acoustic Emission Test for Microelectronic Tape Automated Bonding," Nondestructive Testing Handbook, 2nd edition, Vol. 5, pp. 361-364 (ASNT, 1987).

G. Harman, "Acoustic Emission Thermal Shock Test for Hybrid Microcircuit Packages," Nondestructive Testing Handbook, 2nd edition, Vol. 5, pp. 365-369 (ASNT, 1987).

G. Harman, "Designing Microelectronic Welds for Acoustic Emission Testability," Nondestructive Testing Handbook, 2nd edition, Vol. 5, pp. 409-410 (ASNT, 1987).

A. W. Hartman, "Standards for Particle Size," Proc. International Conf. on Liquid Borne Particle Inspection and Metrology, pp. 109-121 (1987).

P. R. Heyliger, J. C. Moulder, P. J. Shull, M. Gimple, and B. A. Auld, "Numerical Modeling of Capacitive Array Sensors Using the Finite Element Method," Review of Progress in Quantitative Nondestructive Evaluation 7A, pp. 501-508 (1988).

N. N. Hsu, G. Chen, and M. Sansalone, "Characterization of a Piezoelectric Transducer Coupled to a Solid," Proc. 1987 Ultrasonics Symposium, IEEE Cat. #87, CH2492-7, pp. 689-692 (1987).

N. N. Hsu and D. G. Eitzen, "Point Source/Point Receiver Ultrasonic Wave Speed Measurement," Proc. 1987 Ultrasonics International Conference, pp. 509-514 (1987).

L. J. Inglehart, "Photothermal Characterization of Ceramics," Nondestructive Testing of High-Performance Ceramics," pp. 163-176 (American Ceramic Society, 1987).

L. J. Inglehart and E. LeGal La Salle, "Thermal Wave Physics of Insulating Materials," Review of Progress in Nondestructive Evaluation 7A, pp. 231-237 (1988).

A. Ito and T. Kashiwagi, "Measurement Technique for Determining the Temperature Distribution in a Transparent Solid Using Holographic Interferometry," Applied Optics 26, No. 5, pp. 954-958 (1 March 1987).

F. S. Jing, A. W. Hartman, and R. J. Hocken, "Noncontacting Optical Probe," Review of Scientific Instruments 58, No. 5, pp. 864-868 (May 1987).

M. P. Jones and G. V. Blessing, "The Dynamic Poisson's Ratio of a Ceramic Powder During Compaction," Proc. 1987 Ultrasonics Symposium, IEEE Cat. #87, CH2492-7, pp. 587-590 (1987).

M. P. Jones and G. V. Blessing, "Ultrasonic Evaluation of Spray-Dried Ceramic Powders During Compaction," Nondestructive Characterization of Materials II, pp. 139-147 (Plenum, 1987).

M. P. Jones and G. V. Blessing, "Ultrasonic Evaluation of Spray-Dried Ceramic Powders During Compaction," International Advances in Nondestructive Testing 13, W. J. McGonnagle, editor (Gordon & Breach Science Publishers, NY, 1988).

M. P. Jones and G. V. Blessing, "Ultrasonic Evaluation of Spray-Dried Alumina Powder During and After Compaction," Nondestructive Testing of High-Performance Ceramics, pp. 148-155 (American Ceramic Society, 1987).

A. H. Kahn and M. L. Mester, "An Eddy Current Sensor for the Measurement of Resistivity and Temperature of Aluminum Rod during Extrusion Processing," Review of Progress in Quantitative Nondestructive Evaluation 7B, pp. 1599-1605 (1988).

J. Kosko, "Concrete Research at NBS: New Ways to Understand an Old Material," NBS Research Reports, NBS SP 733, pp. 20-22 (Aug. 1987).

H. M. Ledbetter, R. J. Fields, and S. K. Datta, "Creep Cavities in Copper: An Ultrasonic-Velocity and Composite-Modeling Study," Acta Metall. 35, No. 9, pp. 2393-2398 (1987).

P. Lumbroso and C. E. Dick, "X-Ray Attenuation Properties of Radiographic Contrast Media," Med. Phys. 14, No. 5, pp. 752-758 (Sept./Oct. 1987).

M. L. Mester, A. H. Kahn, and H. N. G. Wadley, "Measuring Internal Temperatures of Aluminum Extrusion," Proc. Fourth Intl. Aluminum Extrusion Technology Seminar, pp. 259-265 (Chicago, IL, April 1988).

R. H. Mignogna, P. P. Delsanto, and A. V. Clark, "Energy Distribution for SH-Waves in Slightly Anisotropic Materials," Review of Progress in Quantitative Nondestructive Evaluation 7B, pp. 1375-1382 (1988).

R. K. Miller, D. Dornfeld, A. Hamilton, J. Mitchell, and K. Yee, "Process Monitoring with Acoustic Emission," Nondestructive Testing Handbook, 2nd edition, Vol. 5, pp. 467-511 (ASNT, 1987).

L. Mordfin, "International Standards for Nondestructive Testing," J. Research NBS 92, No. 6, pp. 387-390 (Nov.-Dec. 1987).

L. Mordfin, editor, Mechanical Relaxation of Residual Stresses, ASTM STP 993, 122 pp. (1988).

J. C. Moulder and T. E. Capobianco, "Detection and Sizing of Surface Flaws with a SQUID-Based Eddy Current Probe," J. Research NBS 92, No. 1, pp. 27-33 (Jan.-Feb. 1987).

J. C. Moulder, N. Nakagawa, and P. J. Shull, "Progress in Uniform Field Eddy Current Methods," Review of Progress in Quantitative Nondestructive Evaluation 7A, pp. 147-155 (1988).

M. Nashman and K. J. Chaconas, "The NBS Vision System in the AMRF," J. Research NBS 93, No. 4, pp. 539-544 (July-Aug. 1988).

S. J. Norton, "Mössbauer Imaging," J. Research NBS 92, No. 5, pp. 325-334 (Sept.-Oct. 1987).

R. C. Placious and T. A. Siewert, "Real-Time Radiology Standards: Results of Workshop," Materials Evaluation 45, pp. 1270-1271 (Nov. 1987).

R. S. Polvani, A. W. Ruff, Jr., and E. P. Whitenton, "A Dynamic Microindentation Apparatus for Materials Characterization," J. Testing and Evaluation 16, No. 1, pp. 12-16 (ASTM, Jan. 1988).

R. C. Reno, R. J. Fields, and A. V. Clark, "Crystallographic Texture in Rolled Aluminum Plates: Neutron Pole Figure Measurements," Review of Progress in Quantitative Nondestructive Evaluation 7B, pp. 1439-1445 (1988).

R. Rensberger, "Process Sensor Measures Internal Temperatures in Extruded Aluminum," NBS Research Reports, NBS SP 735, p. 25 (Dec. 1987).

M. Sansalone and N. J. Carino, "Transient Impact Response of Thick Circular Plates," J. Research NBS 92, No. 6, pp. 355-367 (Nov.-Dec. 1987).

M. Sansalone and N. J. Carino, "Transient Impact Response of Thick Circular Plates," J. Research NBS 92, No. 6, pp. 369-381 (Nov.-Dec. 1987).

M. Sansalone, N. J. Carino, and N. N. Hsu, "Transient Stress Wave Interaction with Planar Flaws," Building Research and Practice 16, No. 1, pp. 18-24 (1988).

T. Sato, O. Ikeda, T. Hatsuzawa, and M. Linzer, "Real-Time Evaluation of Wear Particles Using Electromagnetic Forced Rotation and Laser Scattering," Wear 115, No. 3, pp. 273-284 (1987).

R. E. Schramm, A. V. Clark, Jr., D. V. Mitrakovic, and P. J. Shull, "Flaw Detection in Railroad Wheels Using Rayleigh-Wave EMATs," Review of Progress in Quantitative Nondestructive Evaluation 7B, pp. 1661-1668 (1988).

P. J. Shull, J. C. Moulder, P. R. Heyliger, M. Gimple, and B. A. Auld, "Applications of Capacitive Array Sensors to Nondestructive Evaluation," Review of Progress in Quantitative Nondestructive Evaluation 7A, pp. 517-523 (1988).

T. A. Siewert, "Standards for Real-Time Radiography - National Bureau of Standards," Paper Summaries, Real-Time Imaging III Topical Conference, pp. 21-24 (ASNT Fall, 1988).

J. A. Simmons, E. Drescher-Krasicka, H. N. G. Wadley, M. Rosen, and T. M. Hsieh, "Ultrasonic Methods for Characterizing the Interface in Composites," Review of Progress in Quantitative Nondestructive Evaluation 7B, pp. 893-901 (1988).

J. A. Simmons, C. D. Turner, and H. N. G. Wadley, "Vector Calibration of Ultrasonic and Acoustic Emission Transducers," J. Acoust. Soc. Am. 82, No. 4, pp. 1122-1130 (Oct. 1987).

H. N. G. Wadley, "Interfaces: The Next NDE Challenge," Review of Progress in Quantitative Nondestructive Evaluation 7B, pp. 881-892 (1988).

H. N. G. Wadley, A. H. Kahn, Y. Gefen, and M. Mester, "Eddy Current Measurement of Density During Hot Isostatic Pressing," Review of Progress in Quantitative Nondestructive Evaluation 7B, pp. 1589-1598 (1988).

H. N. G. Wadley and J. A. Simmons, "Microscopic Origins of Acoustic Emission," Nondestructive Testing Handbook, 2nd edition, Vol. 5, Section 3, pp. 63-90 (ASNT, 1987).

H. N. G. Wadley, J. A. Simmons, R. B. Clough, F. Biancaniello, E. Drescher-Krasicka, M. Rosen, T. Hsieh, and K. Hirshman, "Composite Materials Interface Characterization, First Progress Report to SDIO," NBSIR 87-3630 (1988).

F. W. Wang, A. J. Bur, R. E. Lowry, and B. M. Fanconi, "Fluorescence Monitoring of Polymer Processing," Polymer Materials Science and Engineering 59 (1988).

F. W. Wang and E. S. Wu, "Cure Monitoring of Epoxy Resins by Fluorescence Recovery After Photobleaching," Polymer Communications 28, pp. 73-75 (Mar. 1987).

M. B. Weppner and M. Young, "Image Processing for Optical Engineering Applications," NBSIR 87-3065, 105 pp. (Apr. 1987).

G. S. White, C. Nguyen, and B. Rawal, "Young's Modulus and Thermal Diffusivity Measurements of Barium Titanate Based Dielectric Ceramics," Nondestructive Testing of High-Performance Ceramics, pp. 371-379 (American Ceramic Society, 1987).

H. T. Yolken, "Intelligent Processing of Materials," MRS Bulletin XIII, No. 4, p. 7 (Materials Research Society, Apr. 1988).

H. T. Yolken, editor, "Nondestructive Evaluation, Technical Activities, 1987," NBSIR 87-3611, 83 pp. (Oct. 1987).

J. H. Zimmerman, "Recommended Technical Specifications for Procurement of Commercially Available Systems for the Inspection Workstation," NBSIR 88-3379, 32 pp. (1988).

4. AWARDS AND APPOINTMENTS

Department of Commerce Silver Medal

The Silver Medal Award is bestowed for "meritorious contributions of exceptional value to the Department." Recipients during FY 1988 included Nicholas J. Carino of the Center for Building Technology. Dr. Carino, who led the development of the impact-echo technique for detecting flaws in concrete structures, was recognized for his outstanding leadership in directing the successful investigation of the structural integrity of the U.S. embassy building in Moscow. Carino was also elected to the title of Fellow of the American Concrete Institute in recognition of his work on nondestructive testing of concrete and his important contributions to several of the Institute's technical committees.

Also honored with a Silver Medal Award was Charles R. Tilford of the Center for Basic Standards. A principal investigator in the NDE Program's leak testing project, Dr. Tilford was cited for his leadership role in developing improved pressure measurement standards. His pioneering development of ultrasonic manometry is the basis of new standards and instrumentation that have become widely used in industry.

Department of Commerce Bronze Medal

The Bronze Medal Award for Superior Federal Service is the highest honorary recognition available for NIST presentation. One of this year's recipients was A. Van Clark, Jr., of the Fracture and Deformation Division, who was honored for his leadership and contributions in NDE of materials and components. Dr. Clark developed a strong group effort in NDE with emphasis on measurements indicative of structural integrity and reliability, which provide the nation with improved means of assessing the safety of buildings, bridges, and industrial facilities.

ISHM Technical Achievement Award

The International Society of Hybrid Microelectronics selected Stanley Ruthberg as one of three recipients of its Technical Achievement Award for 1987. A group leader in the Center for Electronics and Electrical Engineering at the time of his death late in 1986, Ruthberg pioneered the leak testing activities in the NDE Program. The award recognized his long-term and diverse contributions to the technical community, particularly in the area of leak testing of hermetic microelectronic packages.

Special Award for Excellence in Technology Transfer

The Federal Laboratory Consortium for Technology Transfer selected Melvin Linzer of the Metallurgy Division and David S. Kupperman of Argonne National Laboratory to receive one of its special awards. The joint award commends the excellent cooperative effort by NIST, the American Iron and Steel Institute, and Magnaflux Corporation to implement an ultrasonic sensor technology for detecting flaws in hot metal.

AEWG Fellow

Nelson N. Hsu of the Center for Manufacturing Engineering was elected a Fellow of the Acoustic Emission Working Group. Dr. Hsu was cited for his outstanding professional distinction and continued significant contributions to the AEWG and to the advancement of acoustic emission technology.

ASTM E-7 Certificate of Appreciation

ASTM Committee E-7 on Nondestructive Testing established a certificate of appreciation in 1987 to recognize individuals for outstanding contributions to the work of the Committee. Of twenty-eight certificates awarded to date, five have gone to NIST staff: Julius Cohen, Donald G. Eitzen, George W. Free, Barbara Howell, and Leonard Mordfin.

NIST Safety Award

The NIST Safety Award for Superior Accomplishment recognizes unusually significant contributions to the NIST Occupational Safety and Health program activities. The award is presented to individuals and to organizational units. The Office of Nondestructive Evaluation was honored with an organizational award in recognition of an eight-year unblemished safety record.

Community Service Awards

Twenty-seven federal employees of four agencies were honored with desk-top plaques for their involvement in a Boulder, Colorado outreach effort called CARE, for Career Awareness and Resource Education, coordinated by NIST. CARE is aimed at getting students interested in pursuing studies leading to careers in science and technology by providing the students with opportunities to meet and talk with people who work in those areas. Among those honored were Tom Capobianco and Fred Fickett of the Center for Electronics and Electrical Engineering, and Ray Schramm and Peter Shull of the Fracture and Deformation Division, all of whom participate in the NDE Program.

Gerald V. Blessing, Center for Manufacturing Engineering, was elected Technical Vice Chairman for the 1989 International Ultrasonics Symposium of the Institute of Electrical and Electronic Engineers.

Donald G. Eitzen, Center for Manufacturing Engineering, was appointed Chairman of the ASTM/NIST/ASNT symposium on NDE standards, tentatively scheduled for the fall of 1989.

David S. Lashmore, Metallurgy Division, was elected Chairman of the Electrodeposition Division of the Electrochemical Society.

NBS-114A (REV. 2-8C)

U.S. DEPT. OF COMM. **BIBLIOGRAPHIC DATA SHEET** *(See instructions)*	1. PUBLICATION OR REPORT NO. NISTIR 88-3839	2. Performing Organ. Report No.	3. Publication Date OCTOBER 1988

4. TITLE AND SUBTITLE

Nondestructive Evaluation -- Technical Activities - 1988

5. AUTHOR(S)

H. Thomas Yolken, editor

6. PERFORMING ORGANIZATION *(If joint or other than NBS, see instructions)*

National Institute of Standards and Technology

~~NATIONAL BUREAU OF STANDARDS~~

U.S. DEPARTMENT OF COMMERCE

GAITHERSBURG, MD 20899

7. Contract/Grant No.

8. Type of Report & Period Covered

Annual, FY1988

9. SPONSORING ORGANIZATION NAME AND COMPLETE ADDRESS *(Street, City, State, ZIP)*

SAME

10. SUPPLEMENTARY NOTES

☐ Document describes a computer program; SF-185, FIPS Software Summary, is attached.

11. ABSTRACT *(A 200-word or less factual summary of most significant information. If document includes a significant bibliography or literature survey, mention it here)*

A review of the Nondestructive Evaluation Program at NIST for fiscal year 1988 is presented in this annual report.

12. KEY WORDS *(Six to twelve entries; alphabetical order; capitalize only proper names; and separate key words by semicolons)*

acoustic emission; composite materials; eddy currents; materials processing; metal forming; nondestructive evaluation; powders ceramic and metal; radiography; sensors; standards; thermal testing; ultrasonics

13. AVAILABILITY

☒ Unlimited

☐ For Official Distribution. Do Not Release to NTIS

☐ Order From Superintendent of Documents, U.S. Government Printing Office, Washington, D.C. 20402.

☒ Order From National Technical Information Service (NTIS), Springfield, VA. 22161

14. NO. OF PRINTED PAGES

73

15. Price

$13.95